SANDIA REPORT

RECEIVED
MAY 24 2000
OSTI

Contained Rocket Motor Burn Demonstrations in X-Tunnel: Final Report for the DoD/DOE Joint Demilitarization Technology Program

S. W. Allendorf, B. W. Bellow, R. F. Boehm, L. R. Carrillo, J. R. Carson, Y. –T. Chen,
H. Fry, W. C. Gray, S. K. Griffiths, R. L. Heinle, C. J. Hewitt, H. A. Johnsen, A. E. Moeller,
R. H. Nilson, D. K. Ottesen, R. L. Peabody, C. R. Shaddix, A. Smiecinski, J. R. Stephens,
K. J. Stetzenbach, W. C. Thomas, C. A. Velsko, B. E. Watkins, and S. M. Williams

Edited by
J. Lipkin

Sandia National Laboratories

Issued by Sandia National Laboratories, operated for the United States
Department of Energy by Sandia Corporation.

Available to DOE and DOE contractors from
    Office of Scientific and Technical Information
    P.O. Box 62
    Oak Ridge, TN 37831

    Prices available from (703) 605-6000
    Web site: http://www.ntis.gov/ordering.htm

Available to the public from
    National Technical Information Service
    U.S. Department of Commerce
    5285 Port Royal Rd
    Springfield, VA 22161

    NTIS price codes
    Printed copy: A05
    Microfiche copy: A01

DISCLAIMER

**Portions of this document may be illegible
in electronic image products. Images are
produced from the best available original
document.**

Contained Rocket Motor Burn Demonstrations in X-Tunnel: Final Report for the DoD/DOE Joint Demilitarization Technology Program

B. W. Bellow, A. E. Moeller, S. M. Williams
Bechtel Nevada

R. L. Heinle, C.A. Velsko, B. E. Watkins
Lawrence Livermore National Laboratory

C. J. Hewitt, H. Fry, J. R. Stephens
Los Alamos National Laboratory

J. R. Carson, W. C. Gray, W. C. Thomas
Radian International

R. F. Boehm, Y. -T. Chen, A Smiecinski, K. J. Stetzenbach
University of Nevada, Las Vegas

and

S. W. Allendorf, L. R. Carrillo, S. K. Griffiths, H. A. Johnsen,
R. H. Nilson, D. K. Ottesen, R. L. Peabody, C. R. Shaddix,
Sandia National Laboratories

Edited by

Joel Lipkin
Environmental Technologies Applications Department
Sandia National Laboratories
Livermore, CA 94550

ABSTRACT

Three low-pressure rocket motor propellant burn tests were performed in a large, sealed test chamber located at the X-tunnel complex on the Department of Energy's Nevada Test Site in the period May-June 1997. NIKE rocket motors containing double base propellant were used in two tests (two and four motors, respectively), and the third test used two Improved HAWK rocket motors containing composite propellant. The preliminary containment safety calculations, the crack and burn procedures used in each test, and the results of various measurements made during and after each test are all summarized and collected in this document.

ACKNOWLEDGEMENT

Table of Contents

List of Figures

List of Tables

Contained Rocket Motor Burn Demonstrations in X-Tunnel: Final Report for the DoD/DOE Joint Demilitarization Technology Program

Introduction and Background

The Joint Demilitarization Technology (JDT) Program is a collaborative effort between the Departments of Defense and Energy (DoD and DOE) that is demonstrating and validating technologies for resource recovery, recycling, and alternative destruction/treatment technologies. The JDT Program is managed by the Demil Technology Office of the US Army Defense Ammunition Center, McAlester, OK, and the US DOE Nevada Operations Office, Las Vegas, NV. In FY97, the JDT Program completed two test series using the X-tunnel complex in Area 25 at DOE's Nevada Test Site (NTS):

- Phase I testing which included four detonation tests (employing M107 155mm HE projectiles), and
- Phase II testing in which three low-pressure rocket motor propellant burns were executed (employing NIKE and Improved HAWK rocket motors).

Executive summaries describing test procedures and the results obtained from both of these JDT Program phases are given in references (1) and (2), respectively. The present report provides additional background information related to the Phase II test series. In addition, this report serves as a guide to the separate data reports that were prepared by the principal investigators who participated in these tests.

The test facility located in the X-tunnel complex at NTS is a mined cavity (the test chamber) that is sealed off from the access drift by a steel and concrete containment barrier. This barrier was designed to withstand blast effects (e.g., shock, shrapnel impacts, and high pressure/temperature environments) as well as to prevent the release of gases produced by munition detonations and rocket motor propellant burns. The volume of the test chamber is roughly 4644 m³ (164,000 ft³), and its dimensions are roughly 30.5 m long, 15.2 m wide, and 10.7 m high. Containment calculations performed by Burkhard (3) indicate that the test chamber and containment barrier can safely contain a detonation of 3000 pounds of double base propellant (roughly equivalent to 2250 pounds of TNT).

The rocket motor burn tests used two different DoD tactical rocket motors: the NIKE M88 and the Improved HAWK. These motors contain propellants that are representative of the two most common formulations found in the demilitarization inventory, i.e., double base and composite. Each NIKE M88 rocket motor contains 341 kg (750 pounds) of double base type propellant, and each Improved HAWK dual thrust motor contains 294 kg (647 pounds) of composite type propellant.

Three tests were performed: "SUNSPOT" and "THUNDERBIRD" using 2 and 4 NIKE motors, respectively; and "DAZZLER" using 2 Improved Hawk motors. In each test, linear shaped charges and explosive cutting tape were used to split the steel rocket motor cases longitudinally and partially around the circumference. The explosives also served to initiate the low-pressure (i.e., non-propulsive) propellant burns. This procedure closely followed the DoD Open Burning (OB) process generally referred to as "crack and burn". Test parameters are summarized in Table 1.

7

Table 1. Contained rocket motor burn tests in x-tunnel

Test Name	Test Type[1]	Date Executed	Number of Motors	N.E.W.[2] (pounds)	Inert Weight (pounds)
SUNSPOT	B1	14 May 97	2	1500[3]	888
THUNDERBIRD	B1	28 May 97	4	3000[3]	1776
DAZZLER	B2	11 June 97	2	1294[4]	490

1 - B1 = Burn of NIKE rocket motors; B2 = Burn of Improved HAWK rocket motors
2 - Net Explosive Weight (excluding initiating explosive charges)
3 - NC/NG (double base) Propellant
4 - Composite Propellant

Data/Sampling Strategy

Extracted gas and aerosol samples, combined with in situ and post-test measurements, were used to obtain both time-averaged and time-resolved data in each test. Much of the time-averaged data was used to determine concentrations of the analytes of environmental interest in the combustion cloud. The data collection techniques and analyses employed in these tests focused on the following areas:

- laboratory analyses [using U.S. Environmental Protection Agency (EPA) standardized methods] of gas and particulate samples extracted from the combustion cloud—these analyses used to identify the presence of EPA regulated chemicals,
- rapid, time-resolved measurements of selected gas species and aerosol/particulates using both extraction and in situ methods,
- determination of the presence of toxic gases and explosive mixtures in the tunnel complex (as required by health and safety rules at NTS),
- in situ measurements of combustion cloud gas temperature (time histories and spatial variations), and
- time-resolved measurements of gas pressure in the test chamber.

To a large extent, the gases and aerosols produced in each test were contained in the test chamber and sampled over several hours after test initiation. During the sampling period, these gases cooled and nominally returned to atmospheric pressure and temperature.

Species Generated: A number of gases, chemicals and Resource Recovery Act (RCRA) listed hazardous metals were generated during each rocket motor burn test. These included, for example: CO_2, CO, NOx, HCN, HCl, Pb, Cr, products of incomplete combustion [including volatile organic chemicals (VOCs), semi-volatile organic chemicals (SVOCs), dioxins, and furans], residual energetic material, and small aerosols and particulates.

Effluent Measured: Time averaged concentrations of many of the above species were determined by appropriate EPA standard methods. In addition, a few species (bulk gases, NOx, CO, and particulates) were measured using time-resolved methods. Note that dioxins, furans, and HCl were only measured in the DAZZLER test; where their presence was anticipated as a consequence of the combustion of the composite type propellants in the Improved HAWK rocket motor.

Sample Methods: EPA sampling methods were used to collect time-averaged, "grab" samples on the portal side of the containment barrier. This sampling was initiated after

it was determined that the pressure and temperature in the test chamber were below safe limits. The total duration of this sampling was typically 60-120 minutes. Solid residue samples were also collected from the chamber after each test. EPA approved methods were used to analyze these samples and determine their leachability [Toxicity Characteristic Leaching Procedure (TCLP)] properties. Small aerosols and particulate entrained in combustion cloud were also sampled using time-resolved techniques. Bulk gas concentrations were determined in real time using several instruments, including some located at the end of a 300 m long sampling tube running from the test chamber to the tunnel portal. These gas samples were extracted continuously during and after the propellant burns. The analytical instruments used to analyze these gas samples included a mass spectrometer, gas chromatograph, infrared meters, and electrochemical sensors. In addition, in situ, laser-based measurements were made at two sites inside the test chamber. These measurements employed a tunable diode laser with a capability of providing gas phase concentrations of CO_2, CO, HCN, HCl and water in the chamber at a sampling frequency of nominally 1 Hz.

The full suite of measurement types used in the Phase II test series is summarized in Table 2.

Table 2. Sampling and measurements for Phase II test series

Brief Description	Data Summary in Appendix	Responsible Organization*
EPA Standard Methods: VOCs, SVOCs, particulates, metals, HCN, HCl, Dioxins, residual energetic material	A	Radian International, LLC
Real Time Gas Analyses	B	LLNL/ Bechtel Nevada
Real Time and Time-Resolved Aerosol and Particulate Sampling/Analysis	C	LANL
FTIR Gas Species Analysis (see note 1)	D	LANL
Metal Residue Analyses	E	Radian/UNLV
In situ Laser Measurement (see note 2)	F	SNL
Chamber pressure/gas temperature	G	LLNL/Bechtel Nevada

*LANL - Los Alamos National Laboratory
LLNL - Lawrence Livermore National Laboratory
SNL - Sandia National Laboratories
UNLV - University of Nevada, Las Vegas
1 – THUNDERBIRD and DAZZLER only
2 – SUNSPOT and DAZZLER only

Preliminary and Containment Analyses

The theoretical heat of explosion for the double base propellant in the NIKE M88 rocket motor is 764 cal/gm. Similarly, for the composite propellants in the Improved HAWK rocket motor[1], the calculated heats of explosion are 597 and 571 cal/gm for the booster and sustainer grains, respectively. This energy is rapidly released when these propellants burn. The hot combustion products mix with the cool ambient air in the

---

[1] Each Improved Hawk rocket motor is composed of two composite propellant grains: one designated as the booster grain and the other as the sustainer grain.

sealed test chamber, and the temperatures and pressure of all the gases in the chamber increase substantially. In order to insure that these gases would be safely contained, it was necessary to estimate the time histories, and especially the peak values, of pressure and temperature expected in each of the three rocket motor burn tests. Furthermore, even after combustion, the hot gases contained at above atmospheric pressure in the test chamber could be a concern because they represent a source of heat that might weaken the steel components in the containment barrier. Prolonged exposure to these elevated temperatures could also adversely affect any instrumentation located in the test chamber.

Several different numerical simulations of the rocket motor propellants burning in the test chamber were used to obtain these estimates. Nilson and Griffiths (4) developed an analytical model to predict the evolution of the temperature and pressure in a pair of well-mixed control volumes. These volumes were normalized by the volume of the test chamber. In their analysis, it was assumed that each of these volumes has the same pressure but distinct temperatures at any instant, and that the combustion products are released at a uniform rate into the primary control volume, V^*. The temperature, pressure and volume of V^* thus increase during the assumed burn time of $t_b = 20$ seconds. Energy is continuously transferred between control volumes and to the rock walls of the test chamber by buoyancy driven convection, forced convection driven by gas release, and by radiation. All of these energy transfer processes are relatively slow, however, compared to the assumed burn time. For this reason, the peak temperatures and pressures shown in Figures 1 and 2, respectively, for both the NIKE and Improved HAWK rocket motors are determined mainly by the:

- amount of mass and energy released by combustion,
- initial air mass in the test chamber,
- volume of the test chamber, and
- thermodynamic properties of the gases, each taken as ideal with appropriate mean molecular weights and specific heat ratios.

It was assumed that the total energy release was the same as for conventional firing of each motor. That is, no allowance was made for using available oxygen in the test chamber to oxidize the CO produced by combustion to CO_2. For the sake of conservatism, these calculations also assume that the entire test chamber is well mixed (i.e., $V^* = 1.0$). This assumption tends to reduce both the average gas temperature and the cooling rate of the gases in the test chamber. That is, high local temperatures and cooling rates would be expected to occur if the combustion products were not well mixed and instead formed stable stratified layers containing only moderate amounts of entrained air.

This analysis suggests that combustion of the NIKE rocket motors in the SUNSPOT and THUNDERBIRD tests will produce the highest peak pressures and temperatures in the test chamber. These peak values should be achieved at the end of combustion; followed by rapid decreases as the gas in the chamber cools. These predicted temperature and pressure histories for burning 2 and 4 NIKE rocket motors are shown in Figures 3 and 4, respectively, taken from (4). It is evident that the predicted temperature and pressure decay rates shown in Figures 3 and 4 depend strongly on the apparent emissivity, ε^*, of the hot gases in the test chamber. This parameter relates to the efficiency of heat transfer due to radiation (i.e., high emissivity corresponds to enhanced heat loss to the chamber walls). For these calculations, ε^* was assumed to
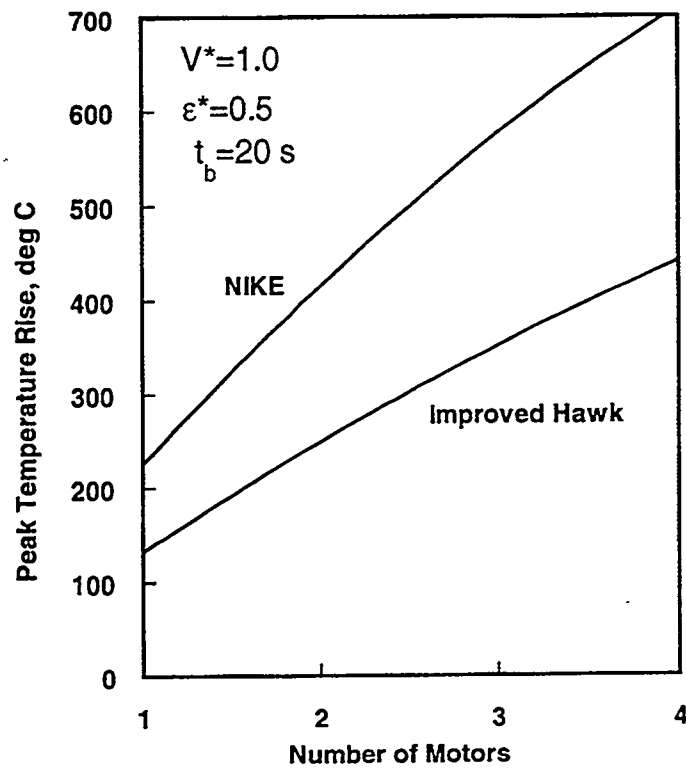
Figure 1. Computed peak temperatures in test chamber, from Ref (4).
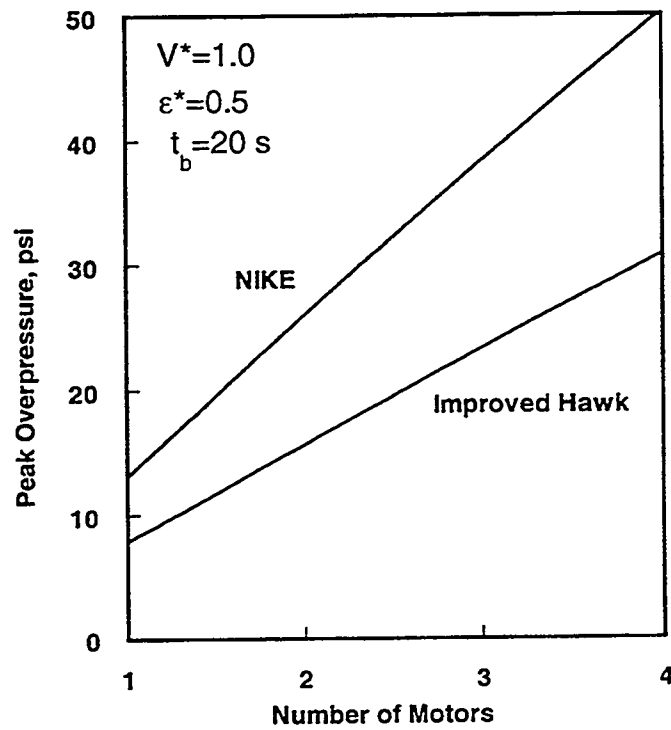
Figure 2. Computed peak pressures in test chamber, from Ref (4).
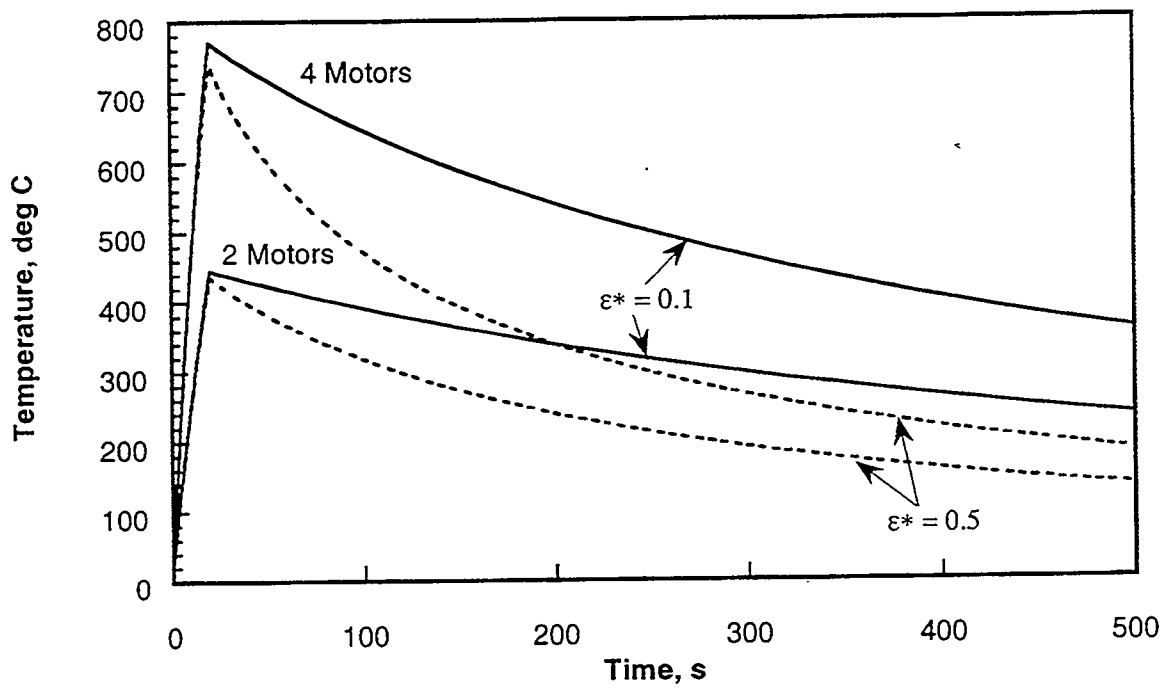
Figure 3. Computed temperature histories for combustion of NIKE rocket motor propellant in test chamber, from Ref (4).
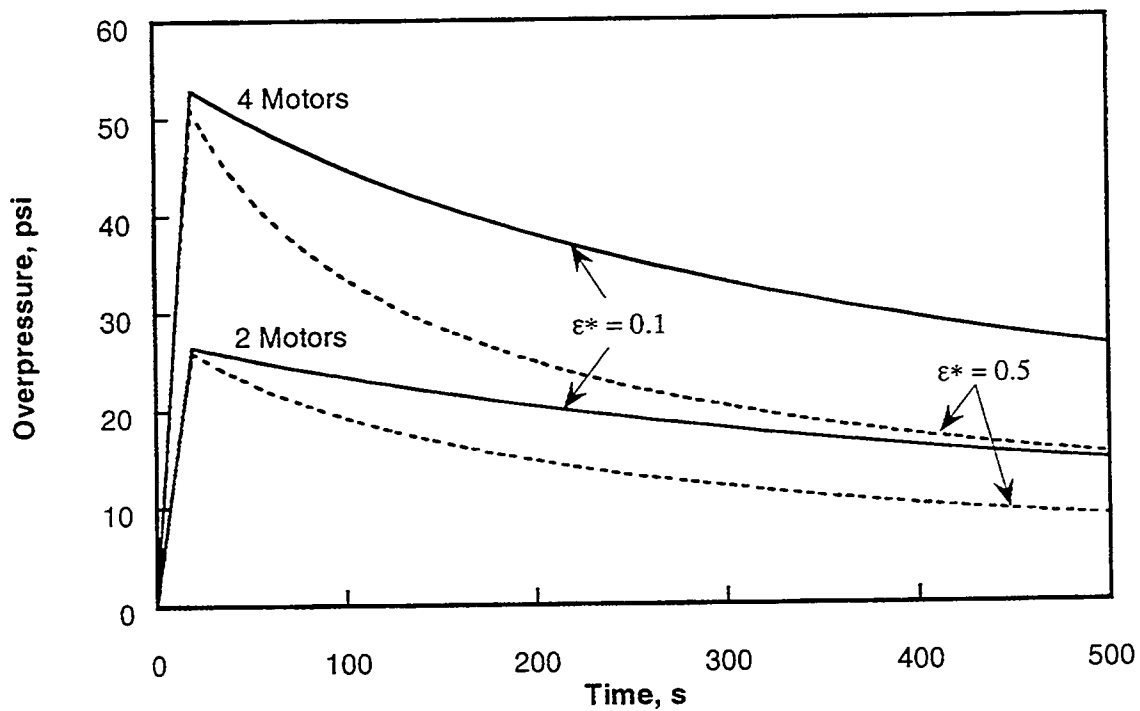
Figure 4. Computed pressure histories for combustion of NIKE rocket motor propellant in test chamber, from Ref (4).

12

be either 0.1 or 0.5 in order to span a reasonable range of potential values for this parameter.

A second analysis of the temperature and pressure histories in the test chamber was carried out by Boehm and Chen (5). They developed a one-dimensional, transient heat transfer model and analyzed both the well mixed and gas stratified cases, focusing especially on results that could be expected for burning a single NIKE rocket motor. They also carried out a parameter sensitivity analysis on their results by using ranges of values for a number of different heat transfer coefficients included in their model. Such a sensitivity analysis was important because exact values of the heat transfer coefficients can not be determined in advance. In the well mixed case, and where parameters overlap, their results are similar to those shown in Figures 1-4 from (4). In the stratified model, where it is assumed that hot gases "pool" at the top of the test chamber during combustion, they calculate that both peak temperature and pressure in the test chamber are substantially reduced compared to the well mixed case. This result follows from the rapid quenching of the hot gases during the stratification process. Further analyses, and an extension of the numerical model in (5) to two-dimensions, can lead to a more thorough understanding of the complex heat transfer processes that occur in the test chamber during rocket motor burn events.

A third analysis that principally addressed containment issues for the rocket motor burn test series was carried out by Burkhard (3). Burkhard used the commercially available computer code, BLASTX (6), to estimate peak static[2] and dynamic loads on the containment barrier in an assumed worst case scenario in which the propellant in 4 NIKE rocket motors detonates rather than burns. The detonation sensitivity of the NIKE rocket motor propellant is sufficiently high to warrant this concern; even though both the geometry of the propellant grain and the methods employed to split the rocket motor cases and initiate the burn make a detonation event very unlikely. An additional feature of the BLASTX code allowed Burkhard to include the effects of oxidizing the CO produced by combustion to CO_2. This exothermic conversion is often referred to as an "after burn" because it proceeds somewhat more slowly than the primary combustion process. With the presence of sufficient O_2 and H_2, however, the CO-to-CO_2 conversion occurs during combustion, as well as for some time thereafter (i.e., as long as temperatures are high enough for the reaction to proceed). Including this "after burn" process has the effect of increasing both the temperature and pressure calculated by BLASTX. The results given in (3) when there is no oxidation of CO agree with the peak values shown in Figures 1-2. These results change dramatically, however, when CO-to-CO_2 conversion is included. For example, the peak static pressure in THUNDERBIRD increases from 51 psig to 129 psig, and the peak temperature increases from roughly 700 °C to 1700 °C. Clearly, for containment safety purposes, the conservative approach is to assume that combustion goes to completion in these tests so that all of the CO generated is converted to CO_2. Pressure and temperature limits for the containment barrier were established using that approach.

A heat transfer calculation was also carried out in (4) to predict the temperature rise of the steel plates in the containment barrier. For this analysis, it was assumed that the combustion cloud gases reached a peak temperature of 1700°C followed by a

---

[2] BLASTX does not account for the combustion gas cooling that occurs due to the action of various heat transfer mechanisms. Therefore, the "static" values for pressure and temperature generated by BLASTX are effectively upper bounds on the peak values computed in (4).

characteristic decay similar to that shown in Figure 3. The results of that calculation indicated that a 0.75 inch thick plate could reach a peak temperature on the order of 130 °C at roughly 1200 seconds after burn initiation. This temperature is well below a thermal softening threshold for structural steel, and thus it was concluded that the thermal cycling history generated by the rocket motor burn tests series would not adversely affect the integrity of the containment barrier.

Test Configurations and Arming and Firing Procedures

In his X-tunnel test summary report (7), Peabody describes all of the test configurations as well as the arming and firing procedures that were used for the Phase I and II tests in X-tunnel. The configurations and procedures for the Phase II rocket motor burn tests are briefly summarized here.

Schematic plan views of the rocket motors in the test chamber for the SUNSPOT, THUNDERBIRD, and DAZZLER tests are show in Figures 5 and 6. Note that the layout shown in Figure 5 is appropriate for both SUNSPOT and DAZZLER since two motors were used in each of these tests. The centers of the layouts shown in Figures 5 and 6 were roughly 19 m from the containment barrier. In each case, the rocket motors were secured to the concrete pad in the test chamber. This procedure prevented them from moving during the burn initiation event and the subsequent propellant burn out. The motors were offset laterally to preclude any possibility of a sympathetic detonation if the propellant in one motor were to detonate as a result of the initiation process.

In addition to using copper linear shaped charges and explosive cutting tape to initiate the propellant burns, separate copper linear shaped charge explosives were used to rapidly open standard sized tanks of compressed inert gases. These gases were released at test initiation time, and they were used as tracers for the real time gas measurements in each test. One bottle of Krypton was used in each of the SUNSPOT and THUNDERBIRD tests, and 2 bottles (1 each of Krypton and Neon) were used in DAZZLER. The weights of all of the explosives used in each test are summarized in Table 3.

Table 3. Explosives used to initiate low-pressure propellant burns*

Explosive Source	SUNSPOT	THUNDERBIRD	DAZZLER
Copper Linear Shaped Charge	250gr/ft X 16=0.571#	250gr/ft X 32=1.143#	250gr/ft X 16=0.571#
Copper Linear Shaped Charge	600gr/ft X 5=0.429#	600gr/ft X 5=0.429#	600gr/ft X 10=0.857#
Explosive Cutting Tape	300g/ft X 10=0.429#	300gr/ft X 20=0.857#	300gr/ft X 13=0.571#
RP1 Detonator (RDX)	0.626g X 6=0.0084#	0.626g X 10=0.014#	0.626g X 8=0.0112#
Total Exp. Weight (lbs)	1.437	2.443	2.010

*Includes copper linear shaped charges used to cut open tanks of compressed inert tracer gas(es)
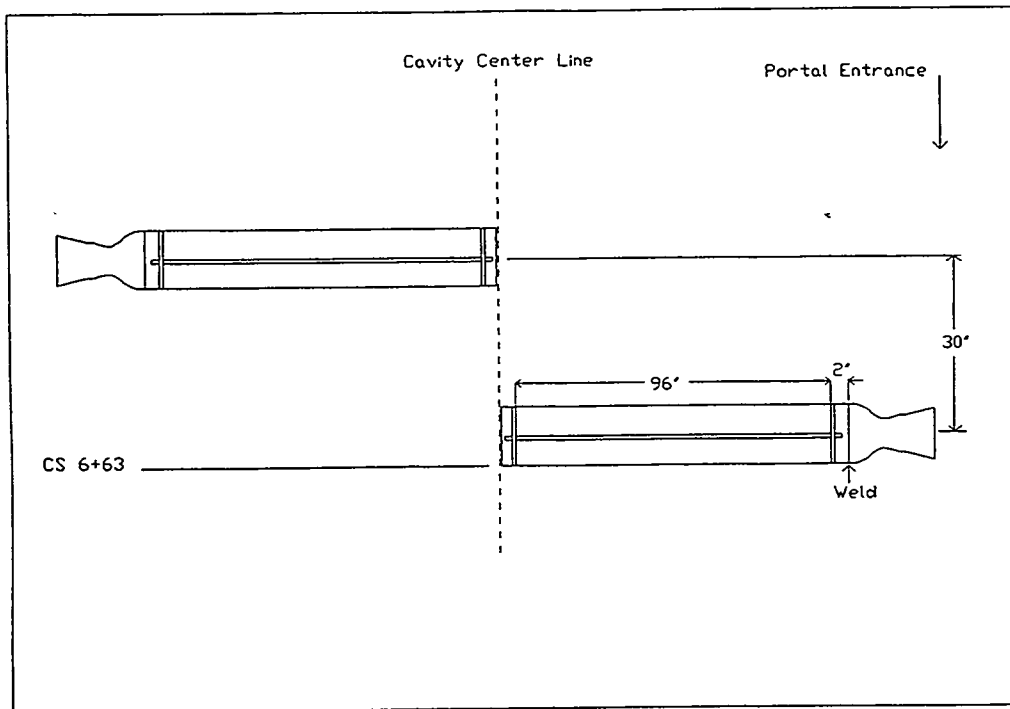
Figure 5. Plan view of rocket motor arrangement for SUNSPOT and DAZZLER tests.
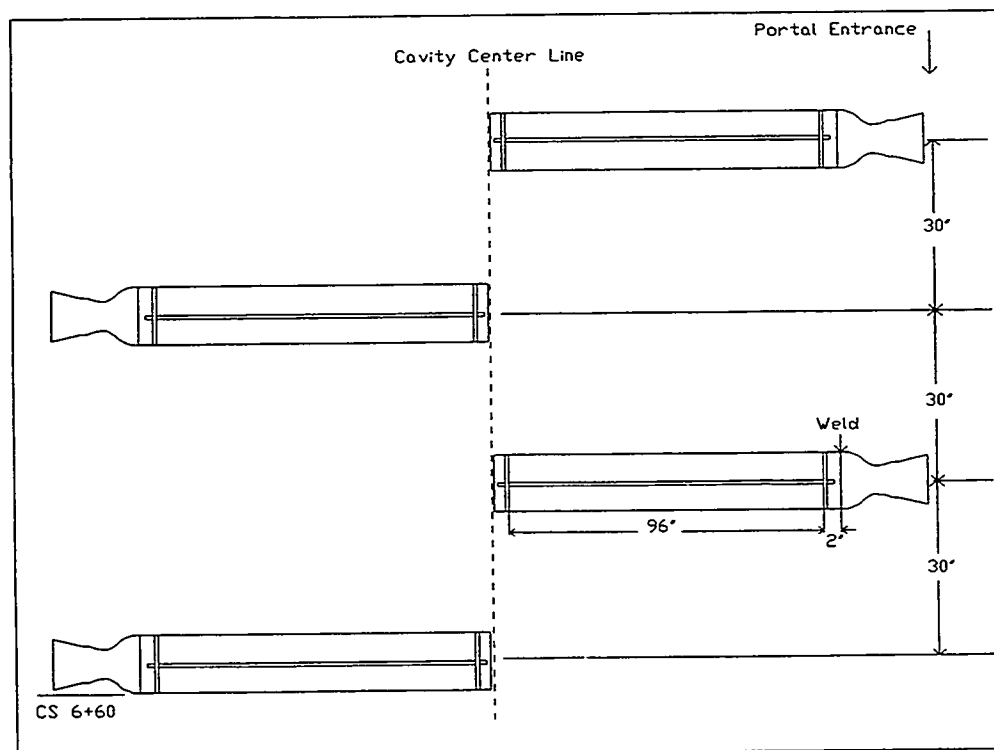
Figure 6. Plan view of rocket motor arrangement for THUNDERBIRD test.

The arrangement of the rocket motors and the initiating explosives as well as the effectiveness of the burning process can be seen in the photographs in Figures 7 and 8. Figures 7a and 8a show the positioning of the motors and the arrangement of the linear shaped charges and explosive cutting tape on the motors prior to the initiation of THUNDERBIRD and DAZZLER, respectively. Similarly, Figures 7b and 8b are views of the spent rocket motor cases after each of these tests. It is evident from Figures 7b and 8b that the rocket motor cases did not move during the initiation and burn processes.

Test Summaries

SUNSPOT

The first rocket motor burn in the X-tunnel test chamber was designated SUNSPOT. This test was conducted on 14 May 1997. The test consisted of cracking and burning two NIKE rocket motors containing a total of 1500 lbs of double base propellant. In addition, a compressed gas cylinder of Krypton was explosively opened simultaneously with the initiation of the burn event. Test initiation time was 1133 hours (PDST).

Instrumentation: With the exception of the FTIR diagnostic, the complete suite of sampling methods and instrumentation given in Table 2 was employed in this test. In addition, a video camera with a view of the test chamber interior was installed behind a port on the chamber barrier at a height of roughly 3 m above the chamber invert (floor).

General Results: Several observations from the SUNSPOT test are reported here, and the data obtained in this test are included in Appendices A-G. From the video record of the burn event and an analysis of the temperature/pressure records, we can identify a short delay (1-3 seconds) between the initiation of the explosives and the start of the propellant burn. The burn itself lasted 20-25 seconds. Peak pressure in the chamber was measured at roughly 56 psia, and it occurred about 41 seconds after test initiation. The time delay between the apparent end of the burn and the measured pressure peak may be evidence of continued CO-to-CO_2 conversion in the combustion cloud. Leaks around the containment barrier into the portal side of the tunnel were observed as pressure in the chamber increased. The particulate-laden gas cloud leaking from the test chamber obscured the view of the video camera focused on the containment barrier within 2-3 minutes after test initiation.

All of the time-resolved instrumentation performed well for the first 2-3 minutes after test initiation. At later times some of the thermocouple junctions failed, probably due to the high water content and acidic nature of the combustion products. In addition, the laser access windows in both TDL detector locations were eventually coated to a point where no laser light could be transmitted across the gas sampling volume. Peak temperatures between 550°C and 1200°C (depending on location) were measured at a time that correlates with the occurrence of peak pressure. These measurements tend to confirm that the combustion cloud gases in the chamber tend to be stratified at early times; with the highest-temperature gases observed roughly 8 m above the invert and 2 m below the chamber back (roof). The sampling ports for the Radian and LANL instrumentation were opened roughly 22 minutes after test initiation due to a concern about the initial high temperatures and pressures observed in the test chamber.
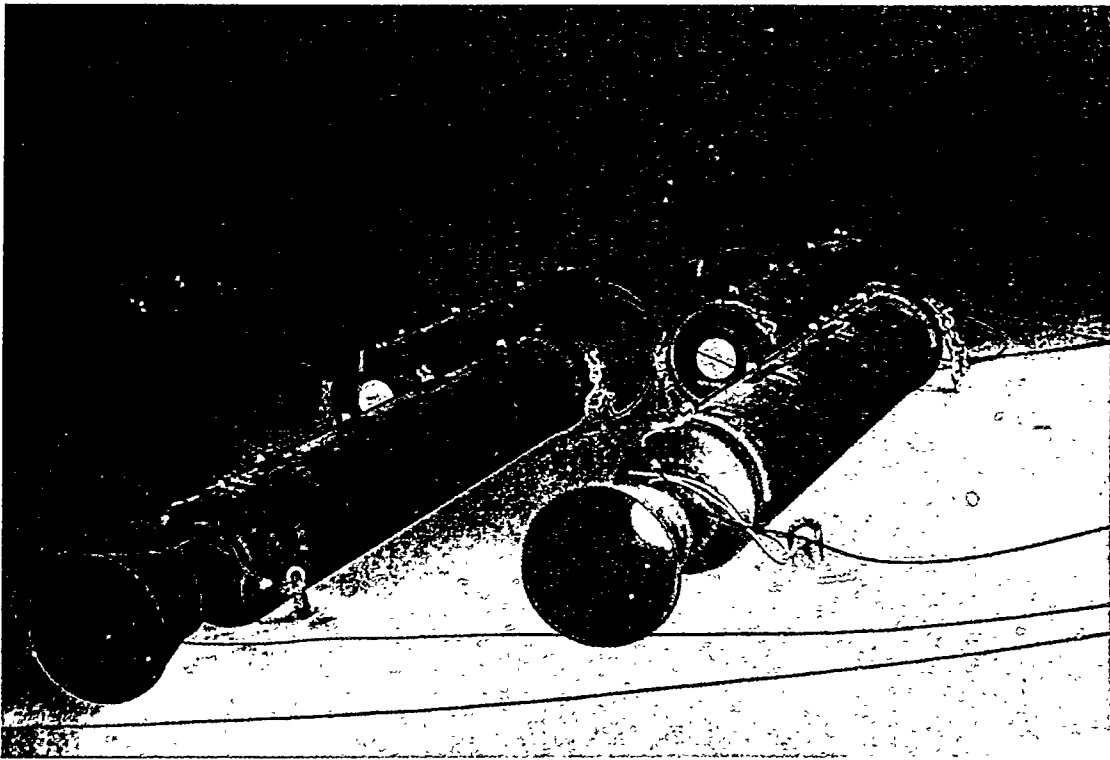
Figure 7a. View of 4 NIKE M88 rocket motors in test chamber prior to THUNDERBIRD.
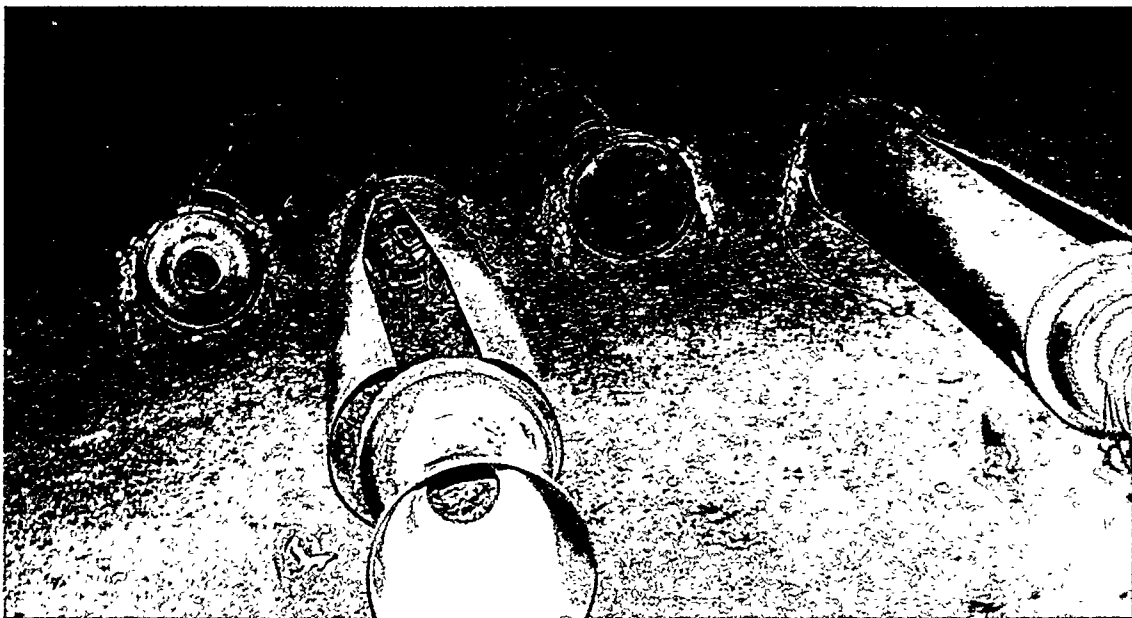
Figure 7b. Remnants of NIKE rocket motor cases after THUNDERBIRD.

Figure 8a. View of 2 improved Hawk rocket motors in test chamber prior to DAZZLER.

Figure 8b. View of improved Hawk rocket motors after DAZZLER.

18

Chamber Reentry: A nominal atmosphere was monitored in the chamber after several gas exchanges over a 12-18 hour period. Reentry commenced at approximately 1030 hours on 15 May. Personnel entering the chamber were protected by tyvex suites and were required to use supplied-air respirators (SCBA). No unburned propellant was found, and the chamber was judged to be clean and relatively dust free. After off-site lab analyses revealed relatively low contamination in the chamber (particularly for lead and asbestos), the personnel protection requirement was reduced to powered air respirators.

THUNDERBIRD

The THUNDERBIRD test was performed 28 May 1997. The test consisted of cracking and burning four NIKE M88 rocket motors containing a total of 3000 lbs of double base propellant. In addition, a compressed gas cylinder of Krypton was explosively opened simultaneously with the initiation of the burn event. Test initiation time was 1100 hours (PDST).

Instrumentation: With the exception of the SNL TDL gas species monitor, the complete suite of instrumentation identified in Table 2 was used in this test. The thermocouple array used in SUNSPOT was modified for this test. The 8-station, invert to back, array was reconfigured to 7 stations with the highest thermocouple located roughly 8 m above the invert. The array was also moved to a new location roughly 18 m from the center of the rocket motors positioned on the concrete pad. These changes were made in an effort to increase the chances of the thermocouple array surviving the high temperature environment in the chamber during THUNDERBIRD. The SNL TDL gas species monitor enclosures were insulated and sealed prior to the execution of THUNDERBIRD.

General Results: Several observations from the THUNDERBIRD test are reported here, and the data obtained in this test are included in Appendices A-G. From the video and temperature records we can see there was a short delay (~ 1 second) between the initiation of the explosives and the start of the propellant burn. The burn itself lasted 20-25 seconds. One anomaly noted on the video, and confirmed on reentry, was that the propellant in one of the 4 motors "burned out" more quickly than that in the others. Burn time on this motor appeared to be less than 10 seconds, and its steel case was split open more than 12 inches compared to a more typical 1-2 inches for the other motors in the test. Peak pressure in the chamber was measured at 85 psia, and it occurred roughly 32 seconds after test initiation. A significant particulate-laden cloud was observed leaking around the chamber barrier, along the invert cable/pipe trenches, and through some of the instrumentation feed-throughs.

Nearly all of the real-time instrumentation performed well during THUNDERBIRD. Gas sampling from the top of the chamber was curtailed a few minutes after test initiation due to an apparent failure of the filter on that sampling line. Six of the seven thermocouples recorded stable temperature profiles well into the chamber cool down phase. Maximum temperatures of between 650°C and 800°C were recorded depending on location. The sampling ports for the Radian and LANL instrumentation were opened approximately 10 minutes after burn initiation due to a concern about the initial high temperatures and pressures in the test chamber. Some clogging of the filters on these sampling lines due to the heavy particulate loading in the chamber reduced the total sampling time.

Chamber Reentry: A nominal atmosphere was monitored in the chamber after several gas exchanges over night. On reentry no unburned propellant was found, and the chamber was judged to be clean and relatively dust free. The results obtained from subsequent lab analysis of contamination in the chamber (especially lead and asbestos) allowed the personnel protection requirement to be reduced to powered air respirators for x-tunnel test chamber operations required prior to DAZZLER.

DAZZLER

The DAZZLER test was the final rocket motor burn test performed in X-tunnel. DAZZLER was executed on 11 June 1997, and it consisted of cracking and burning two Improved HAWK rocket motors in the test chamber. The total weight of the composite propellant contained in these motors was 1294 lbs. In addition, cylinders of compressed gas, one each of Krypton and Neon, were explosively opened simultaneously with the initiation of the burn event. Test initiation time was 1100 hours (PDST).

Instrumentation: Monitoring and instrumentation for this test included the complete suite of air emission and temperature/pressure monitors identified in Table 2. Two of the thermocouples in the 7-station thermocouple array used in THUNDERBIRD were replaced, and the array was reinstalled at essentially the same location in the test chamber.

General Results: Several observations from the DAZZLER test are reported here, and the data obtained in this test are included in Appendices A-G. The first 10-12 seconds of the propellant burn was captured on the video record. The video viewing port was obscured after this time due to aluminum deposition on the surface of the glass. For this reason, the exact burn time is somewhat uncertain. The pressure peaked at roughly 42 psia and at a time of 30 seconds after test initiation. No gas leaks were noted on the portal side of the containment barrier.

All of the real-time instrumentation performed well during DAZZLER. Maximum temperatures between 500°C and 575°C were recorded on the thermocouple array, depending on location. The sampling ports for the Radian and LANL instrumentation were opened approximately 5 minutes after burn initiation. Some clogging of the filters on these sampling lines due to the heavy particulate loading in the chamber reduced the total sampling time.

Chamber Reentry: A nominal atmosphere was monitored in the chamber after several gas exchanges over night. On reentry no unburned propellant was found, and it was noted that the chamber invert was uniformly covered with a thin layer of what appeared to be aluminum oxide particulate. There was also evidence of this powdery coating on the TDL windows and the video viewing port. Analyses of the hazards in the test chamber allowed the use of powered air respirators during subsequent clean-up and shut-down operations at the X-tunnel complex.

Summary of Instrumentation and Sampling/Analysis Procedures

All of the sampling methods and instrumentation used in these tests are described in this section: abstracted data obtained for each test can be found in appendices A-G, and complete data sets are available in the referenced documents.

Time-Averaged Measurements—Radian International, LLC (Appendix A)

Radian was contracted to use EPA methods to obtain time-averaged samples that were subsequently analyzed using EPA laboratory procedures. Results of their measurements are given in Appendix A where species concentrations are expressed as either ppbv or mg/m^3 at a standard pressure of 29.92 inches Hg and 68 °F. A detailed report can be obtained from the author.

The samples Radian extracted from the combustion cloud were analyzed for:

- total suspended particulates (TSP),
- particulate matter with an aerodynamic diameter ≤ 10 μm (PM_{10}),
- volatile organic compounds (VOCs),
- semivolatile organic compounds (SVOCs),
- polychlorinated dibenzo-p-dioxins/polychlorinated dibenzofurans (PCDD/PCDF) (DAZZLER test only),
- hydrogen chloride (HCl)/chlorine (Cl_2) (DAZZLER test only),
- metals, and
- hydrogen cyanide (HCN).

In addition, post-test residue samples were collected and analyzed for:

- residual energetics and other organic compounds to assess destruction effectiveness, and
- metals (total and leachable).

The metals analysis of the residue helped provide information about appropriate waste disposal of debris from the test chamber. Two types of samples were collected for residue analyses: solid samples that settled out of the combustion cloud and were recovered from 4 separate, 1 m^2 areas on the horizontal surface of the concrete pad, and residue washed from the surfaces of 2 aluminum plates using a water and alcohol mixture. These plates were positioned vertically in the test chamber, roughly 3 m above the invert, and they had a total surface area of 0.75 m^2.

The gas samples Radian extracted from the combustion cloud passed through several hollow probes that went into the test chamber through the containment barrier. These probes were isolated from their sampling equipment by remotely operated valves that were closed prior to test initiation. The isolation valves were only opened after it is determined that the temperature and pressure in the test chamber are within safe limits for the sampling equipment. Nominal safe temperature and pressure limits were set at 100°C and 50 psig, respectively. As noted above, these valves were opened at roughly 22, 10 and 5 minutes after test initiation in SUNSPOT, THUNDERBIRD, and DAZZLER, respectively. The delay in opening the sampling valves for SUNSPOT was excessive, and that delay most likely compromised the quality of the time averaged data Radian and LANL obtained in that test. The observation of inconsistent temperature data reported from the thermocouples the test chamber during SUNSPOT was the source of this 22 minute delay. The problem was resolved in THUNDERBIRD and DAZZLER by revising the thermocouple array location and by using a dedicated thermocouple located near the sampling ports in the test chamber.

In some cases, Radian acquired replicate samples because the heavy particulate loading of the combustion clouds in these tests could cause some of the samples collection trains to be voided. For those situations where replicate samples were

collected and analyzed, the replicate results were averaged together to calculate a single result for the test. If an analyte was detected in one sample but not detected in a replicate sample, the nondetected sample was ignored in calculating the average result for the test.

Time-Resolved Bulk Gas Analyses—LLNL/Bechtel Nevada (Appendix B)

Results obtained from the bulk gas sampling of the combustion products generated in these tests are summarized in Appendix B. A detailed description of the measurement procedures and data analyses used is given in (8). Continuous analysis of gas extracted from the test chamber—as well as discrete sampling into 1-liter containers for post-test analysis at LLNL—were used to determine time-resolved[3] combustion cloud gas compositions in each test. These data were also analyzed to calculate carbon balances for each test.

On-line composition analyses of the gas samples extracted from the test chamber were obtained for each test. Where possible, duplicate measurements were made in an effort to ensure that viable composition data were obtained. Measurements for product gases were also obtained from two different types of instruments as an internal check on performance. These instruments were located in the "Mobile Noble" trailer positioned on the apron outside the tunnel portal. The gas samples from the test chamber were piped into the trailer where the line pressure was regulated manually. The gas samples were then distributed to the various analytical measurement units in the trailer. Several different continuous emission monitors sampling the incoming gas for CO, CO_2, O_2, NO_2, and NOx were accessible for reading the displays or changing meter ranges. The gas chromatograph (GC), sample processor lines, and quadrupole mass spectrometer (QMS) made up the other main unit in the trailer. All equipment associated with the Mobile Noble gas analysis trailer was computer controlled. A Macintosh running Labview was used for the QMS, and another Macintosh interfaced all the vacuum and sampling hardware. An IBM-type PC monitored and maintained a log file of Mobile Noble control actions for each experiment, and was also used to log the data from the NOx and CO monitor. A laptop PC controlled and recorded data from the portable GC.

Real-Time and Time-Averaged Aerosol Analyses—LANL (Appendix C)

The Los Alamos Aerosol Sampling System (LAASS) was specially developed to measure aerosol concentrations as well as to collect aerosol samples during these tests. After the propellant burn was complete in each test, sampling port valves were opened remotely and the LAASS collected representative aerosol samples from the combustion cloud. These samples were obtained by drawing aerosol-laden gas through the containment barrier into two parallel sampling systems. One system (impactor) was used to collect aerosol samples from 0.1 to 10 µm in aerodynamic diameter and measure their mass concentrations ($\mu g/m^3$) in real time. The second system (streaker) collected three aerosol size fractions, > 10 µm, 2.5 - 10 µm, and < 2.5 µm. The latter two size fractions were collected on rotating substrates thereby providing a time history of the aerosols in the test chamber. The streaker samples were subsequently analyzed using Proton-Induced X-ray Emission (PIXE) Spectroscopy to determine the aerosol

---

[3] The finite transit time for a gas sample from the test chamber to reach the on-site analytical instrumentation introduces an essentially constant time shift of roughly 2 minutes between the test initiation time and the time-resolved concentration measurements obtained by these techniques.

elemental composition for elements with atomic numbers greater then 11. Data obtained from the LAASS instrument are summarized in Appendix C. A summary report describing the LAASS instrument and its performance in these tests is available from the author.

The impactor is a cascade impactor that separates particles by aerodynamic diameter into 7 size bins with particle separation points of 10, 5, 2.5, 1.2, 0.6, 0.3, and 0.12 μm. Particles larger than the separation points are successively removed as the air stream passes through the collector. Particle mass at each stage is measured by depositing the particles onto quartz crystal micro-balances (QCMs) that change frequency as particles are deposited on them. QCM frequencies are recorded every second in the LAASS. The rate of frequency change with time at the set mass flow rate is a measurement of aerosol mass concentration ($\mu g/m^3$) for each size bin.

The streaker collector separates particles by aerodynamic size with separation points of 10 and 2.5 μm. Particles larger than 10 μm are collected on a fixed collector while particles between 2.5 and 10 μm are collected on a moving impact surface. Particles less than 2.5 μm are collected on a moving filter. The streaker sampler thus collects a time series of aerosol samples that are analyzed using the PIXE analytical technique for elemental concentrations. The chemical state, or solid phases, within the particles is not measured. Operating the streaker and impactor collectors in conjunction allows both size distributions and high quality samples to be obtained for analysis.

Each sampler is attached to a 100 mm diameter flange and tube that penetrates the containment barrier. A high pressure and temperature 50 mm barrier valve, located on the low pressure side of the barrier, isolates each sampling system from the atmosphere in the test chamber. From each sampling valve a 50 mm diameter sampling probe penetrates through the barrier and extends 0.6 m into the chamber to isolate the sampled air from the chamber walls. In order to insure that the LAASS instrument remains within its design limits, the barrier valves are not opened until the gas temperature and pressure in the test chamber fall below 200°C and 100 psig, respectively. For the rocket motor tests, the barrier valves were opened and the first sample taken at 27, 19, and 10 minutes after the ignition time for the SUNSPOT, THUNDERBIRD, and DAZZLER tests, respectively. Because of the high particle levels experienced in these tests, it was necessary to operate the samplers in a "grab sample" mode. That is, samples were taken for short periods (<5 minutes) every 10-15 minutes for at least one hour after test initiation.

LAASS operations were controlled by a multi-level computer system. A programmable logic controller (PLC) was located in a purged cabinet on the portal side of the containment barrier. The PLC controlled the operation of the valves and flow controllers, and collected data from the aerosol and other sensors. The PLC was in turn controlled by a computer located in the instrumentation trailer that was situated outside the tunnel portal. The PLC and controlling computer are connected by fiber optic lines that were used to transmit both the LAASS instrument commands and the measured data.

Real-Time Gas Species Analyses Using FTIR—LANL (Appendix D)

A Fourier Transform Infrared Spectroscopy (FTIR) diagnostic was deployed for analyzing the gas species that evolved during the THUNDERBIRD and DAZZLER rocket motor burn tests. This diagnostic was designed and deployed on a short time

scale during the third quarter of FY97 principally to detect and quantify the evolution of the HCl gas that was generated in the DAZZLER test.

The effectiveness of the FTIR diagnostic depends on the design of the sampling system and its ability to provide a representative sample. The system in X-tunnel was implemented so that a gas sample extracted from the test chamber would only have to travel a relatively short distance to the instrument's absorption cell. The FTIR cell itself was chosen to be 10 cm long in order to provide optimum detection of HCl at concentrations of 2 % mole fraction. The system was designed to minimize sampling effects by using teflon tubing which provides less wall reaction and absorption than steel. The tubing for the longest run of the sample line—roughly 30 m—was 12.5 mm diameter to minimize its surface-to-volume ratio. Based on previous experience, the system was also designed to use a flow rate of 28.3 l/min to minimize wall effects during sampling. A cyclone filter is included to remove particles larger than 10 μm. In addition, a sintered metal filter downstream of the cyclone filter removed particles larger than 0.5 μm. Finally, the sample line and FTIR absorption cell were heated to minimize the effects of water condensation. The sample line was also instrumented with pressure transducers and flow meters to assess system performance remotely. Data obtained from the FTIR diagnostic instrument are summarized in Appendix D. A summary report describing the FTIR diagnostic instrument and its performance in these tests is available from the author.

Post-Test Metal Residue Analyses—UNLV (Appendix E)

The Harry Reid Center for Environmental Studies at the University of Nevada, Las Vegas (UNLV) was contracted to analyze water/alcohol (50/50) rinse samples collected by Radian International. These samples were taken from two aluminum coupons (plates) that were exposed to the combustion clouds in the test chamber. The total surface area of the coupons was 0.75 m^2. The coupons were cleaned before each test and fixed vertically in the chamber at a height of roughly 3 m above the invert (floor). After exposure to the combustion cloud, the coupons were recovered and washed down with the water/alcohol mixture that UNLV analyzed. Samples were dried, digested, and analyzed using EPA method 200.8 (ICP-MS). The analyses were preformed using an Inductively Coupled Plasma Mass Spectrometer (ICP-MS). In this way, UNLV was able to identify metal residues that collected on the surface of the aluminum during each test. The results of these analyses are given in Appendix E.

In Situ, Laser-Based Measurements of Gas Species Concentrations—SNL (Appendix F)

A modified commercial gas monitor based on tunable diode laser (TDL) spectroscopy was used to make in situ, real time measurements of several gas species in the test chamber during the SUNSPOT and DAZZLER rocket motor burn tests. The development, installation and application of the TDL gas monitoring system were the responsibilities of SNL. A detailed description of this diagnostic method and its performance in these tests is given in (9). A summary of the results obtained from it is included in Appendix F.

The TDL monitor employed in this application operates in the near-infrared portion of the electromagnetic spectrum; and it detects molecular species using optical absorption by vibration transitions in overtone and combination modes at wavelengths near 1.30 μm and 1.55 μm. The monitor is capable of providing the time-varying concentrations of

two different gas species in the test chamber (i.e., using two separate TDL modules). These data are obtained essentially simultaneously and in real time at a sampling rate on the order of 1 Hz. For the rocket motor burn tests, the gas species monitored included HCN, CO/CO_2 and H_2O. A TDL monitoring system of this type is especially suitable for detecting reactive gases because it can provide gas species concentration measurements that are in-situ (i.e., no sample extraction required) and probe free. Along with the gas species concentration measurements, the TDL monitors also provide quantitative, time-resolved information about the particulate loading in the combustion clouds produced by the rocket motor burns. This occurs because the intensity of TDL near-infrared light that reaches the detector is proportional to the particulate size and concentration in the portion of the combustion cloud continuously sampled by the monitor.

Two fixed sites in the test chamber were chosen for installation of the TDL detectors and sampling volumes. One site was located in the invert of the chamber, and a second site was built into the rib (side wall) of the chamber at a height of 4.9 m above the invert location. Both sites were roughly 15 m from the working point of the rocket motor burn tests. The path length of the TDL "light" for each of the two monitors in each sampling volume was 0.5 m. The TDL modules themselves (i.e., the laser light sources) and their associated electronic control hardware and data logging computer were located in the instrumentation trailer on the apron outside the X-tunnel portal. Suitably modulated light from the modules was transmitted to the sampling volumes in the test chamber using commercial, communications-grade optical fibers. The low-voltage electrical signals generated by the TDL light detectors at the measurement sites contain the transmitted laser power and gas species concentration data. These signals were returned to the instrumentation trailer using coaxial cable.

Time-Resolved Measurements of Test Chamber Pressure and Temperature—LLNL and Bechtel Nevada (Appendix G)

LLNL and Bechtel NV were responsible for measuring and recording a variety of physical parameters in each test. Data obtained from these measurements are summarized in Appendix G. Complete data sets are available from the author.
In addition to early-time shock, ground motion and strain gage measurements on the containment barrier, the data for each test included temperature measurements from a linear array of K-type thermocouples and the gas pressure history in the test chamber. These data were recorded prior to test initiation (baseline data) and for roughly two hours after the propellant burn was complete. Long-term data were sampled at 1-Hz using the NTS Special Measurements Integrated Data System (SMIDS). Both the rapid rise and relatively slow decay in pressure and the transient gas temperatures associated with the propellant burning and the gas cool down after the burn were recorded in this way. Depending on the test, there were seven or eight thermocouples in a thermocouple array. These thermocouples were equally spaced in the array in an effort to measure gas temperature as a function of height in the test chamber. The array was positioned between the invert and the back of the test chamber for SUNSPOT and between the invert and the mid-height of the chamber in THUNDERBIRD and DAZZLER.

Comparison of Measured Data with Containment Analyses: As described previously, prior to the execution of these tests, three different numerical simulations were used to predict the peak pressures and temperatures that might be expected in

the test chamber (3-5). Figures 9 and 10 show comparisons of the calculated temperature and pressure histories, respectively, for THUNDERBIRD [from reference (4)] with the measured data from that test. These comparisons suggest that the analytical heat transfer models developed in references (4) and (5) provide reasonable simulations of the gross effects of propellant combustion and subsequent gas cooling in the nominally sealed test chamber. The discrepancies that do exist, however, can be qualitative explained by limitations in both the simulations and measurements. An example is the failure to include the heat release associated with CO-to-CO_2 conversion in the simulation. As discussed above, this conversion tends to increase both the gas temperature and pressure in the chamber. A pressure increase is evident (as shown in Figure 10), but a corresponding significant temperature increase is not apparent (Figure 9). We speculate, however, that the location of the thermocouple array in THUNDERBIRD did not permit an unambiguous measurement of the actual peak temperature in that test. This suggestion is consistent with temperature measurements in SUNSPOT where an invert-to-back thermocouple array location made it clear that early-time temperature histories tend to be spatially non-uniform in the chamber. A second discrepancy that can be noted in the comparisons show in Figures 9 and 10 relates to the cooling rate of the gases in the test chamber. The measured temperature and pressure profiles for THUNDERBIRD both indicate that the hot gasses in the chamber cooled more rapidly than predicted. This observation can be reconciled if we speculate that the actual emissivity of the gases is higher than assumed in the calculations. Such a speculation is reasonable since it was necessary to treat the magnitude of the combustion gas emissivity as an unknown parameter in the simulations carried out in references (4) and (5).

Summary and Conclusions

These tests provided a unique opportunity to identify propellant combustion processes and effluents from full-scale rocket motor burns both in real time and by capturing representative products for subsequent analysis. In general, we feel that the time resolved and time averaged data in Appendices A-G reveal important information about those effluents. However, several operational difficulties should be recognized when reviewing these results. These difficulties include:

- the quality of the time-averaged data from Radian and LANL measurements for the SUNSPOT test is likely compromised due to the delayed opening of the valves that isolated their equipment from the test chamber, making it difficult to compare gas and particulate data sampling results between the two NIKE rocket motor tests (SUNSPOT and THUNDERBIRD);
- some measurements of non-volatile compounds obtained for THUNDERBIRD and DAZZLER are ambiguous due to cross contamination from the residues of previous tests in the chamber—the UNLV test methods and residue measurements are least affected by this problem; and
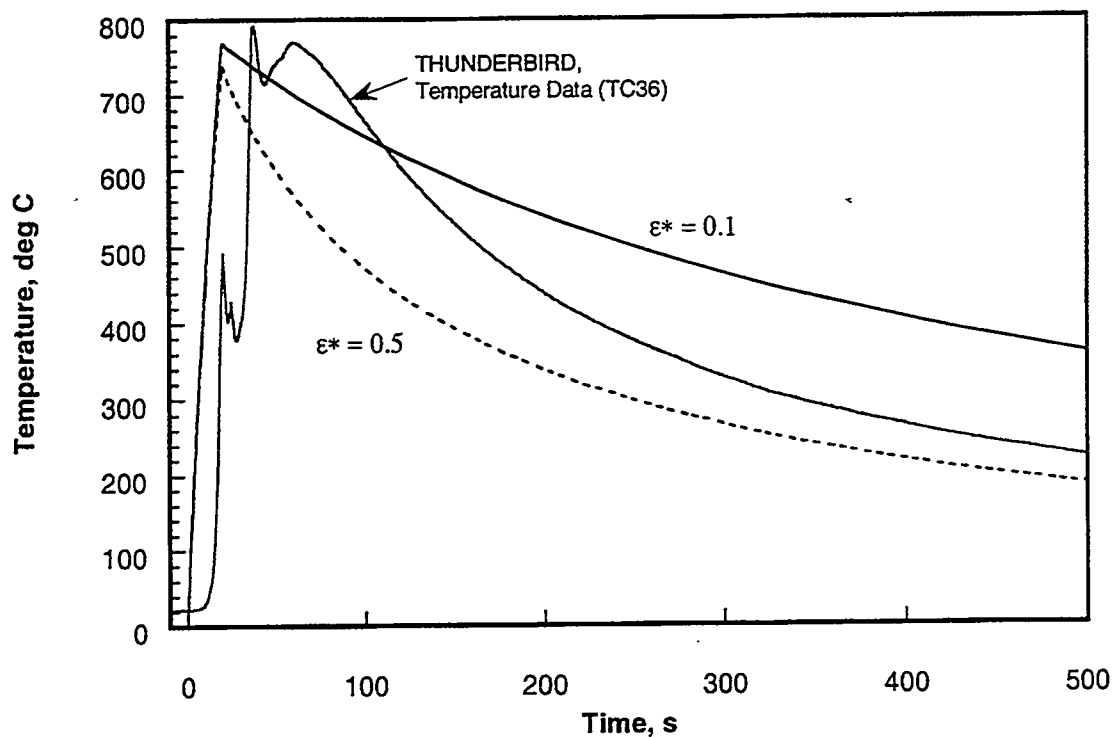
Figure 9. Overlay of computed temperature history for THUNDERBIRD [from Ref (4)] with data from TC36 (thermocouple located 6.4 m above the test chamber invert).
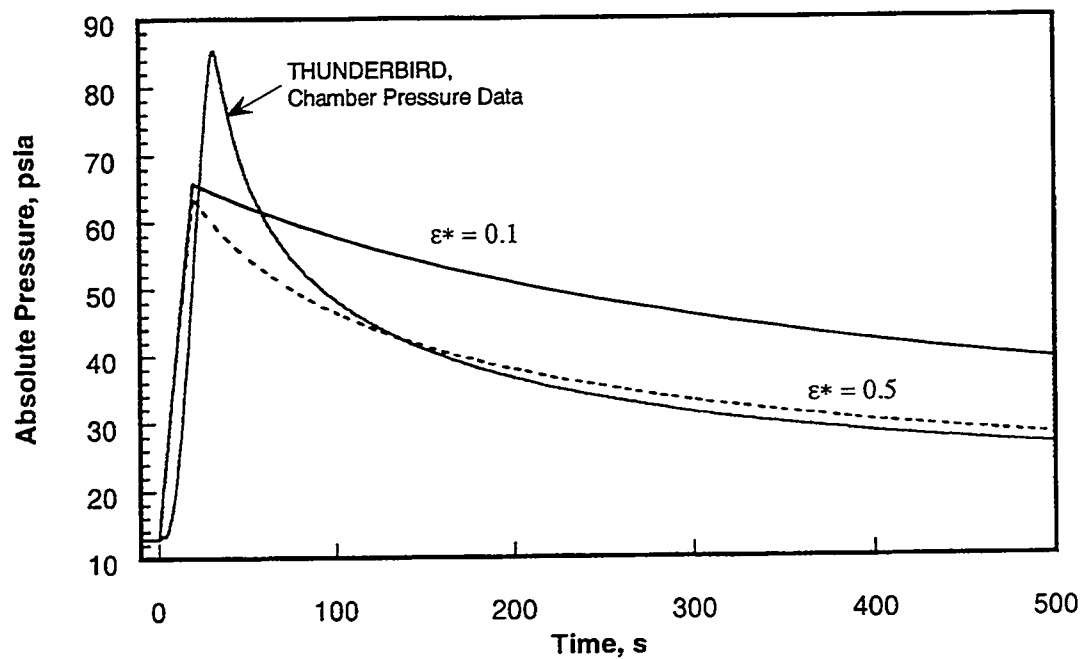
Figure 10. Overlay of computed pressure history for THUNDERBIRD [from Ref (4)] with test data.

- there is evidence that the leak paths that developed between the test chamber and the tunnel drift during SUNSPOT and THUNDERBIRD allowed an in flow of fresh air into the test chamber—it is likely that these gas leaks substantially reduced measured bulk gas concentrations in the test chamber at late times (i.e., greater than about 80 minutes after test initiation)(10).

Nevertheless, the data provided by these tests are an invaluable source of information on the OB process. In addition, it is likely that further analyses of these data can be used to improve the execution and understanding of future munition testing campaigns in X-tunnel.

The data in Appendices A-G indicate that significant amounts of some organic and inorganic compounds are emitted when double base and composite rocket motor propellants are burned. In addition, the combustion clouds generated in these events are characterized by high concentrations of particulates and aerosols. Nevertheless, the carbon balance data summarized in Appendix B, and the residue analyses in Appendix A, suggest that there was nearly complete combustion in each of these tests. We therefore conclude that the crack and burn demilitarization procedure followed by low pressure propellant combustion are safe, efficient and relatively clean disposal operations for excess rocket motors.

References

1. "Executive Summary of Phase I Demonstrations: Detonation of Conventional Weapons: 155-mm High-Explosive M107 Projectiles", Lawrence Livermore Laboratory Report # UCRL-ID-131252, July 1998

2. "Executive Summary of Phase II Demonstration: The Low-Pressure Rocket Motor Burns in X-tunnel", Sandia National Laboratories Report #SAND2000-8202, January 2000

3. "Safety Factors and Design Criteria for U25x Complex (BANSHEE)", July 1996; and "NIKE Rocket Motor Burns – Revised", April 1997, N. Burkhard, Lawrence Livermore National Laboratories, Memoranda to Distribution

4. R. Nilson and S. Griffiths, Sandia National Laboratories, Private Communication, 1996-1997

5. "Analysis Support for the Sandia Rocket Burn Project", R. Boehm and Y.-T. Chen, University of Nevada Las Vegas Contract Report, February 1997

6. "Internal Blast and Thermal Environmental for Internal and External Explosions: A User's Guide for the BLASTX Code, Version 3.0", J. Britt and M Lumsden, Science Applications International Corp., SAIC 405-94-2, May 1994

7. "Final A&F Report on FY1997 Demil Tests at X-tunnel", R. Peabody, Sandia National Laboratories A&F Report AF706, August 1997

8. "Gas Sampling and Analysis Results for Low-Pressure Burn Demilitarization of Rocket Motors", C. Velsko, Lawrence Livermore Laboratory Report # UCRL-ID-136582, December 1998

9. "Tunable Diode Laser Spectroscopy: Report on JDT Contained Rocket Motor Burn Tests", S. W. Allendorf, et al., Sandia Report SAND98-8247, September 1998.

10. "Chamber Leakage Effects on Measured Gas Concentrations During Contained Demilitarization Test at NTS X-Tunnel", C. R. Shaddix and J. Lipkin, Sandia Report, SAND2000-8209, December 1999.

This page intentionally left blank

APPENDIX A

Time-Averaged Measurements—Radian International, LLC

Data obtained by Radian International LLC from post-test, laboratory analyses of samples extracted from the test chamber are summarized in Tables A1-A7. Particulate, HCN, and metal species concentrations in the combustion clouds for SUNSPOT and THUNDERBIRD (NIKE rocket motor tests) are summarized in Table A1. Table A2 summarizes measured concentrations of these same analytes, plus HCl and Cl_2, for DAZZLER (Improved HAWK rocket motor test).

Total nonmethane hydrocarbons and selected VOC concentrations for the NIKE and Improved HAWK rocket motor tests are presented in Tables A3 and A4, respectively. The VOCs presented in these tables were detected at concentrations >15 ppbv in the NIKE tests and > 5 ppbv in the Improved HAWK test. These cutpoints for inclusion in Tables A3 and A4 were chosen because they represent levels nominally five times greater than the sample detection limit.

Tables A5 and A6 present results for SVOCs for the NIKE and Improved HAWK rocket motor tests, respectively. Table A7 presents the PCDD and PCDF results for the Improved HAWK rocket motor test. Also included in Table A7 is the calculated 2,3,7,8-TCDD toxicity equivalence of the sample. These toxic equivalencies were calculated using procedures contained in Appendix IX of 40 CFR 266.

Table A1. Particulate Matter, HCN, and metal concentrations —NIKE rocket motor

Compound	Concentrations, mg/m^3		
	SUNSPOT	THUNDERBIRD	Average
Particulates			
TSP	9.08E+02	1.36E+03	1.13E+03
PM$_{10}$	7.22E+01	4.84E+02	2.78E+02
HCN	2.63E+01	N/A	2.63E+01
Metals			
Average Concentrations >1.0E+02			
Lead	2.58E+02	2.86E+02	2.72E+02
Antimony	1.42E+02	9.88E+01	1.21E+02
Average Concentrations >1.0E+01 but <1.0E+02			
Phosphorus	4.36E+01	5.13E+01	4.75E+01
Calcium	1.52E+01	3.07E+01	2.30E+01
Potassium	4.75E+00	3.52E+01	2.00E+01
Iron	1.03E+01	2.71E+01	1.87E+01
Sodium	4.97E+00	1.66E+01	1.08E+01
Average Concentrations >1.0E+00 but <1.0E+01			
Cadmium	6.88E+00	7.84E+00	7.36E+00
Aluminum	4.74E+00	6.61E+00	5.68E+00
Zinc	3.57E+00	6.72E+00	5.14E+00
Copper	3.65E+00	4.72E+00	4.19E+00
Magnesium	2.27E+00	4.42E+00	3.34E+00
Titanium	1.02E+00	1.92E+00	1.47E+00
Average Concentrations >1.0E-01 but <1.0E+00			
Chromium	2.03E-01	3.22E-01	2.62E-01
Manganese	1.14E-01	2.73E-01	1.94E-01
Barium	1.30E-01	2.20E-01	1.75E-01
Nickel	1.12E-01	1.45E-01	1.28E-01
Strontium	8.86E-02	1.64E-01	1.26E-01
Average Concentrations >1.0E-02 but <1.0E-01			
Arsenic	7.83E-02	9.52E-02	8.67E-02
Selenium	3.38E-02	5.48E-02	4.43E-02
Molybdenum	3.90E-02	3.09E-02	3.50E-02
Cobalt	1.63E-02	2.56E-02	2.09E-02
Vanadium	1.51E-02	1.35E-02	1.43E-02
Mercury	5.84E-03	2.05E-02	1.32E-02
Beryllium	4.54E-03	1.61E-02	1.03E-02

N/A = not available

Table A2. Particulate Matter, HCN, HCl, Cl_2, and Metal Concentrations —Improved HAWK rocket motor

Compound	Concentrations, mg/m³ DAZZLER
Particulates	
TSP	1.18E+03
PM_{10}	1.04E+03
HCN	ND
HCl	1.43E+04
Chlorine	1.13E+02
Metals	
Average Concentrations >1.0E+01	
Aluminum	3.17E+02
Lead	1.92E+01
Iron	1.04E+01
Average Concentrations >1.0E+00 but <1.0E+01	
Copper	7.42E+00
Antimony	4.28E+00
Sodium	2.71E+00
Potassium	1.45E+00
Phosphorus	1.26E+00
Chromium	1.06E+00
Average Concentrations >1.0E-01 but <1.0E+00	
Calcium	8.60E-01
Zinc	6.22E-01
Titanium	3.78E-01
Nickel	2.78E-01
Cadmium	2.02E-01
Magnesium	1.65E-01
Manganese	1.29E-01
Average Concentrations >1.0E-02 but <1.0E-01	
Vanadium	4.53E-02
Molybdenum	3.95E-02
Thallium	2.81E-02
Cobalt	2.19E-02
Barium	1.77E-02
Average Concentrations <1.0E-02	
Mercury	5.93E-03
Strontium	3.11E-03
Silver	2.42E-03
Selenium	2.32E-03
Beryllium	8.13E-04

ND = not detected

Table A3. Selected VOC Concentrations —NIKE rocket motors

Compound	Concentrations, ppbv		
	SUNSPOT	THUNDERBIRD	Average
Average Concentrations >1.0E+04			
Total Nonmethane Hydrocarbons	2.91E+04	9.18E+04	6.04E+04
Acetone	5.96E+03	4.63E+04	2.61E+04
Ethanol	3.82E+03	2.94E+04	1.66E+04
Benzene	1.07E+04	1.66E+04	1.36E+04
Acetaldehyde	7.14E+03	1.98E+04	1.35E+04
Average Concentrations >1.0E+03 but <1.0E+04			
Chloromethane	1.08E+04	6.64E+03	8.69E+03
Acetonitrile	4.69E+03	9.29E+03	6.99E+03
Propylene	1.82E+03	6.13E+03	3.97E+03
Chloroethane	1.25E+03	5.45E+03	3.35E+03
Benzaldehyde	1.08E+03	2.37E+03	1.72E+03
1-Butene/Isobutene	5.56E+02	2.60E+03	1.58E+03
Average Concentrations >1.0E+02 but <1.0E+03			
Naphthalene	1.14E+03	7.70E+02	9.55E+02
Acrylonitrile	1.42E+03	4.61E+02	9.40E+02
2-Butanone	3.01E+02	1.44E+03	8.68E+02
1-Butanol	5.15E+02	1.22E+03	8.67E+02
Methylene chloride	1.88E+01	1.58E+03	7.97E+02
Toluene	5.21E+02	1.02E+03	7.72E+02
Chlorobenzene	3.89E+02	4.14E+02	4.02E+02
Vinyl acetate	1.56E+02	5.77E+02	3.66E+02
trans-2-Butene	1.06E+02	5.04E+02	3.05E+02
Propane	1.16E+02	4.58E+02	2.87E+02
Vinyl chloride	2.85E+02	1.76E+02	2.30E+02
Diethyl ether	1.97E+02	2.42E+02	2.20E+02
cis-2-Butene	7.21E+01	3.39E+02	2.05E+02
Butyraldehyde	1.31E+02	2.26E+02	1.78E+02
Ethylbenzene	5.63E+01	2.11E+02	1.33E+02
n-Butane	4.98E+01	1.85E+02	1.17E+02
m/p-Xylene	6.08E+01	1.49E+02	1.05E+02

34

Table A3. (Continued)

Compound	Concentrations, ppbv		
	SUNSPOT	THUNDERBIRD	Average
Average Concentrations>1.0E+01 but <1.0E+02			
Styrene	ND	9.96E+01	9.96E+01
Butyl acrylate	5.88E+01	9.66E+01	7.77E+01
1,4-Dioxane	8.50E+01	6.24E+01	7.37E+01
o-Xylene	3.70E+01	8.90E+01	6.30E+01
1-Hexene	2.89E+01	9.69E+01	6.29E+01
1-Pentene	2.54E+01	9.96E+01	6.25E+01
Isoheptane	2.27E+01	9.56E+01	5.91E+01
Chloroform	6.60E+00	8.02E+01	4.34E+01
1,2,4-Trimethylbenzene	3.69E+01	4.89E+01	4.29E+01
Chlorodifluoromethane	7.93E+01	4.65E+00	4.20E+01
2-Propanol	3.66E+01	3.38E+01	3.52E+01
Isobutane	1.55E+01	4.93E+01	3.24E+01
o-Dichlorobenzene	2.25E+01	3.92E+01	3.08E+01
trans-2-Pentene	9.92E+00	5.11E+01	3.05E+01
Hexanal	2.70E+01	2.68E+01	2.69E+01
1-Propanol	2.09E+01	3.02E+01	2.55E+01
1-Heptene	1.02E+01	3.93E+01	2.47E+01
n-Pentane	1.04E+01	3.40E+01	2.22E+01
Average Concentrations>1.0E+01 but <1.0E+02 (cont.)			
2-Methyl-1-pentene	2.17E+01	ND	2.17E+01
Cyclopentene	1.10E+01	3.00E+01	2.05E+01
1-Decene	ND	1.93E+01	1.93E+01
1,2-Dichloroethane	1.91E+01	ND	1.91E+01
Methylcyclopentene	ND	1.79E+01	1.79E+01
1,2,4-Trichlorobenzene	1.70E+01	ND	1.70E+01
3-Methyl-1-butene	6.44E+00	2.52E+01	1.58E+01
m-Ethyltoluene	9.67E+00	2.09E+01	1.53E+01
cis-2-Pentene	4.87E+00	2.35E+01	1.42E+01
n-Hexane	7.49E+00	1.57E+01	1.16E+01
1-Octene	5.12E+00	1.74E+01	1.12E+01
n-Heptane	4.71E+00	1.78E+01	1.12E+01
n-Propylbenzene	5.80E+00	1.63E+01	1.10E+01
1-Nonene	5.43E+00	1.61E+01	1.07E+01
Average Concentrations >1.0E+00 but <1.0E+01			
trans-2-Hexene	3.64E+00	1.61E+01	9.87E+00

ND = not detected

35

Table A4. Selected VOC Concentrations—Improved HAWK rocket motor

Compound	Concentrations, ppbv DAZZLER
Average Concentrations >1.0E+03	
Methylene chloride	1.46E+03
Total Nonmethane Hydrocarbons	2.57E+03
Concentrations >1.0E+02 but <1.0E+03	
Benzene	5.62E+02
Ethanol	2.69E+02
Acetaldehyde	1.87E+02
Chloromethane	1.86E+02
2-Propanol	1.44E+02
Acetonitrile	1.41E+02
Acetone	1.33E+02
1-Butanol	1.16E+02
Concentrations >1.0E+01 but <1.0E+02	
Carbon tetrachloride	9.46E+01
Propylene	8.56E+01
Chloroform	7.85E+01
Isobutane	6.62E+01
Benzaldehyde	6.50E+01
Tetrachloroethene	6.47E+01
Propane	6.13E+01
Toluene	5.63E+01
Vinyl chloride	3.13E+01
o-Dichlorobenzene	2.76E+01
Chlorobenzene	2.74E+01
Acrylonitrile	2.64E+01
Isopentane	2.38E+01
Naphthalene	2.14E+01
Butyraldehyde	2.13E+01
n-Butane	2.01E+01
Chloroethane	2.00E+01
m/p-Xylene	1.92E+01
1-Butene/Isobutene	1.62E+01
Trichloroethene	1.12E+01
Concentrations >1.0E+00 but <1.0E+01	
1,2-Dichloropropane	9.70E+00
1-Propanol	9.56E+00
1,2-Dichloroethane	7.92E+00
2-Butanone	7.62E+00
n-Pentane	7.43E+00
Chlorodifluoromethane	7.42E+00
Ethylbenzene	6.96E+00
Benzyl chloride	6.70E+00

Table A5. SVOC Concentrations —NIKE rocket motor

Compound	Concentrations, mg/m³		
	SUNSPOT	THUNDERBIRD	Average
Average Concentrations >1.0E+01			
Diethylphthalate	9.46E+01	4.63E+01	7.05E+01
2-Nitrophenol	1.85E+01	2.04E+01	1.95E+01
Average Concentrations >1.0E+00 but <1.0E+01			
Phenol	1.21E+00	1.20E+01	6.58E+00
Benzoic acid	5.66E+00	6.44E+00	6.05E+00
4-Nitrophenol	3.59E+00	6.94E+00	5.27E+00
Naphthalene	7.06E+00	1.85E+00	4.45E+00
2,4-Dinitrophenol	ND	3.45E+00	3.45E+00
Dimethylphthalate	2.26E+00	3.85E+00	3.06E+00
Acetophenone	1.27E+00	3.55E+00	2.41E+00
Dibenzofuran	2.48E+00	1.43E+00	1.96E+00
Average Concentrations >1.0E-01 but <1.0E+00			
Nitrobenzene	3.37E-01	6.67E-01	5.02E-01
Phenanthrene	4.79E-01	1.11E-01	2.95E-01
bis(2-Ethylhexyl)phthalate	3.88E-01	8.45E-02	2.36E-01
2-Methylnaphthalene	3.18E-01	1.41E-01	2.29E-01
Chrysene	2.16E-01	ND	2.16E-01
1,2-Dichlorobenzene	2.37E-01	1.28E-01	1.82E-01
1,2,4-Trichlorobenzene	1.65E-01	ND	1.65E-01
4-Methylphenol/3-Methylphenol	7.47E-02	1.59E-01	1.17E-01
Benzyl alcohol	1.10E-01	ND	1.10E-01
1,4-Dichlorobenzene	1.02E-01	ND	1.02E-01
1,3-Dichlorobenzene	1.01E-01	ND	1.01E-01
Average Concentrations >1.0E-02 but <1.0E-01			
Fluoranthene	8.70E-02	ND	8.70E-02
2,4,6-Trichlorophenol	ND	7.49E-02	7.49E-02
2-Chlorophenol	3.10E-02	1.17E-01	7.42E-02
Benzo(b)fluoranthene	7.30E-02	ND	7.30E-02
Benzo(k)fluoranthene	7.30E-02	ND	7.30E-02
Fluorene	7.23E-02	2.66E-02	4.95E-02
1,2,4,5-Tetrachlorobenzene	2.30E-02	ND	2.30E-02
Di-n-butylphthalate	1.87E-02	1.99E-02	1.93E-02
Acenaphthylene	1.68E-02	ND	1.68E-02
Anthracene	1.39E-02	ND	1.39E-02
Average Concentrations >1.0E-03 but <1.0E-02			
Pyrene	6.18E-03	ND	6.18E-03

ND = not detected

37

Table A6. SVOC Concentrations —Improved HAWK rocket motor

Compound	Concentrations, mg/m^3 DAZZLER
Concentrations>1.0E+00	
Benzoic acid	1.43E+00
Diethylphthalate	1.05E+00
Concentrations >1.0E-01 but <1.0E+00	
2-Nitrophenol	9.44E-01
2,4,6-Trichlorophenol	6.56E-01
1,2-Dichlorobenzene	3.30E-01
Naphthalene	2.81E-01
Hexachlorobenzene	2.40E-01
Pentachlorobenzene	1.94E-01
4-Nitrophenol	1.60E-01
Concentrations >1.0E-02 but <1.0E-01	
1,2,4,5-Tetrachlorobenzene	9.68E-02
Phenol	8.46E-02
Dibenzofuran	7.58E-02
1,2,4-Trichlorobenzene	6.10E-02
Dimethylphthalate	6.00E-02
4-Chloro-3-methylphenol	4.46E-02
2-Chloronaphthalene	4.36E-02
2,4-Dichlorophenol	4.13E-02
1,3-Dichlorobenzene	3.53E-02
Hexachlorobutadiene	3.47E-02
2-Chlorophenol	3.37E-02
4,6-Dinitro-2-methylphenol	3.35E-02
1,4-Dichlorobenzene	1.94E-02
Phenanthrene	1.03E-02

Table A7. PCDD and PCDF Concentrations—Improved HAWK rocket motor

Compound	Concentrations, mg/m^3 DAZZLER
Polychlorinated dibenzo-p-dioxin	
2,3,7,8-TCDD	7.60E-05
1,2,3,7,8-PeCDD	1.20E-04
1,2,3,4,7,8-HxCDD	8.46E-05
1,2,3,6,7,8-HxCDD	1.42E-04
1,2,3,7,8,9-HxCDD	1.47E-04
1,2,3,4,6,7,8-HpCDD	4.95E-04
1,2,3,4,6,7,8,9-OCDD	1.11E-03
Total TCDD	1.86E-03
Total PeCDD	1.35E-03
Total HxCDD	1.49E-03
Total HpCDD	8.82E-04
Polychlorinated dibenzofurans	
2,3,7,8-TCDF	1.62E-03
1,2,3,7,8-PeCDF	1.05E-03
2,3,4,7,8-PeCDF	7.52E-04
1,2,3,4,7,8-HxCDF	3.32E-03
1,2,3,6,7,8-HxCDF	9.04E-04
2,3,4,6,7,8-HxCDF	7.09E-04
1,2,3,7,8,9-HxCDF	1.92E-04
1,2,3,4,6,7,8-HpCDF	4.81E-05
1,2,3,4,7,8,9-HpCDF	2.55E-03
1,2,3,4,6,7,8,9-OCDF	9.62E-05
Total TCDF	1.38E-02
Total PeCDF	8.56E-03
Total HxCDF	1.01E-02
Total HpCDF	1.30E-02
2,3,7,8-TCDD Toxicity Equivalence[a]	1.31E-03

[a]Calculated using procedures in Appendix IX of 40 CFR 266.

Samples of solid residue collected from the concrete pad on the invert of the test chamber after each test were analyzed for energetics, SVOC's and metals. These data are summarized in Tables A8-A11. Table A8 summarizes the results of the residue energetics analyses. SVOCs found in the residue samples are summarized in Table A9.

The concentrations of metals found in the residue samples are summarized in Table A10. The results of subjecting the residue to the Toxicity Characteristic Leaching Procedure (TCLP) are summarized in Table A11. For the residue from the SUNSPOT and THUNDERBIRD test burns, all the TCLP metals were detected at a level lower than their respective regulatory levels. For the DAZZLER residue, cadmium and lead from the TCLP exceeded the regulatory level for defining the material as "toxic." Since the total metals concentrations of cadmium and lead were similar in all residue samples, the TCLP results for the DAZZLER residue were somewhat unexpected. A possible explanation for the greater leachability of cadmium and lead from the DAZZLER residue is the high HCl content of the combustion gases from the DAZZLER test. Some of the HCl undoubtedly was absorbed on the residue. The acidity associated with the HCl could have caused the metals in the residue to be more readily leached by the TCLP.

Table A8. Energetics in residue samples

Analyte	Concentration, ppb		
	SUNSPOT	THUNDERBIRD	DAZZLER
Octahydro-1,3,5,7-tetranitro-1,3,5,7-tetrazocine (HMX)	ND	ND	411
Hexahydro-1,3,5-trinitro-1,3,5-triazine (RDX)	14950	7350	ND
1,3,5-Trinitrobenzene	ND	ND	1040
2-amino-4,6-dinitrotoluene	ND	ND	20
Net Explosive Weight (NEW), lb	1501.6	3002.8	1211

ND = not detected

Table A9. SVOCs in residue samples

SVOC	Concentration in Residue Samples, µg/kg		
	SUNSPOT	THUNDERBIRD	DAZZLER
2,4-Dinitrophenol	2020	1130	903
2-Methylnaphthalene	98	80	168
2-Nitrophenol	2550	5150	1540
4,6-Dinitro-2-methylphenol	205	ND	ND
4-Nitrophenol	2080	8540	1360
Anthracene	37	ND	ND
Benzo(b)fluoranthene	959	ND	ND
Benzoic Acid	852	999	3410
bis(2-Ethylhexyl)phthalate	4450	283	1040
Butylbenzylphthalate	1410	ND	ND
Chrysene	2270	ND	ND
Dibenzofuran	998	359	302
Diethylphthalate	87500	15500	44200
Dimethylphthalate	1710	657	3620
Di-n-butylphthalate	513	82	ND
Fluoranthene	368	15	ND
Fluorene	51	ND	ND
Hexachlorobutadiene	65	ND	ND
Naphthalene	288	480	90
Nitrobenzene	ND	58	ND
Phenanthrene	728	50	106
Phenol	11100	3930	ND

ND = not detected

41

Table A10. Total metals in residue samples

Metal	Concentration in Residue Samples, mg/kg		
	SUNSPOT	THUNDERBIRD	DAZZLER
Aluminum	NR	NR	19500
Antimony	2370	514	993
Arsenic	9.5	14.2	4.37
Barium	291	169	110
Beryllium	ND	0.464	ND
Cadmium	121	53.7	87.3
Cobalt	5.23	7.04	2.95
Chromium	42	24.7	68.9
Lead	14800	5880	8770
Manganese	283	176	163
Mercury	0.429	0.114	0.435
Nickel	23.5	11.0	12.2
Phosphorus	2360	1050	983
Selenium	1.89	1.15	1.44
Silver	ND	0.207	0.254
Thallium	1.39	2.18	1.04
Zinc	208	140	344

ND = not detected
NR = not reported

Table A11. TCLP metals analysis of residue samples

Metal	Concentration in Residue Leachate, mg/L			Regulatory Level, mg/L
	SUNSPOT	THUNDERBIRD	DAZZLER	
Arsenic	0.049	0.0185	0.007	5
Barium	0.237	0.215	0.313	100
Cadmium	0.0325	0.001	1.94	1
Chromium	0.0035	ND	0.0985	5
Lead	2.80	0.155	29.0	5
Mercury	0.0063	ND	0.00065	0.2
Selenium	0.0075	ND	ND	1
Silver	ND	ND	ND	5

ND = not detected

This page intentionally left blank

APPENDIX B

Time-Resolved Bulk Gas Analyses—LLNL/Bechtel Nevada

An inventory of the propellant and explosive materials consumed in each rocket motor burn test is shown in Table B1. This inventory indicates the carbon content of these materials. All of the carbon-bearing materials in each test must be identified in order to calculate the final distribution of carbon (i.e., the carbon balance) in all of the gaseous combustion products that were measured by LLNL and BN.

Assuming that the low pressure burns in the test chamber represent complete combustion, we can use the inventory information in Table B1 to estimate how much of each product gas will be produced in a given test. The calculated moles of the product gases are shown in Table B2 along with the quantities of inert tracer gas released in each test. Note that the results given in Table B2 generally depend on the assumptions that are made about the composition of the reaction products in a test. For example, the bottom two rows in Table B2 show how two different assumptions on the formation of HCl and Cl_2 affect the calculated moles of H_2O and O_2 in DAZZLER.

The combustion product gas concentrations expected for each test are obtained by using the estimated gas quantities in Table B2 and the initial gas composition in the test chamber. These concentrations are shown in the column labeled *"Expect"* in Table B3. Table B3 also includes a summary of all of the bulk gas species concentration data measured in the rocket motor burn test series.

Table B1. Inventory of materials consumed in rocket motor burns*.

Item Description	Test ID		
	SUNSPOT	**THUNDERBIRD**	**DAZZLER**
Total weight of carbon-containing materials	1606 lb, (2 NIKE) (29.34 wt% carbon)	3212 lb, (4 NIKE) (29.34 wt% carbon)	1334 lb (2 Imp. HAWK) (14.11 wt% carbon)
carbon-containing materials in each motor	OIO propellant, cellulose acetate liner	OIO propellant, cellulose acetate liner	composite propellant, liner, insert
RDX in Copper Linear Shaped Charge (CLSC) (for rocket mtr)	250gr/ft x 16=0.571lb	250gr/ft x 32=1.143lb	250gr/ft x 16=0.571lb
RDX in CLSC (for gas btl)	600gr/ft x 5=0.429lb	600gr/ft x 5=0.429lb	600gr/ft x 10=0.857lb
RDX in Cutting Tape	300g/ft x 10=0.429lb	300gr/ft x 20=0.857lb	300gr/ft x 13=0.571lb
RDX in RP1 Detonator	0.626g x 6=0.0084lb	0.626g x 10=0.014lb	0.626g x 8=0.0112lb
Total RDX Weight ($C_3H_6O_6N_6$)	1.437 lb	2.443 lb	2.010 lb

*From R. L. Peabody, Sandia National Laboratories, Albuquerque, NM, and SPIA Data Sheets and T. Moore, Chemical Propulsion Information Agency, John Hopkins University, MD.

Table B2. Expected rocket burn combustion products and tracer gas amounts.*

Test ID	Test Weight, lbs	H_2O, moles	N_2, moles	CO_2, moles	O_2,** moles	Neon, moles	Krypton, moles
SUNSPOT	1606	12095	3018	17796	-11277		412
THUNDERBIRD	3212	24186	6033	35590	-22553		379.8
DAZZLER (HCl)	1334	12107	2530	7115	-6830	446	380.8
DAZZLER (Cl₂)	1334	13755	2530	7115	-7654	446	380.8

* Assume all metals are completely oxidized (i.e., PbO, Al_2O_3, Fe_3O_4), all nitrogen goes to N_2, all CO goes to CO_2, all hydrogen goes to H_2O or H_2O and HCl [in DAZZLER (HCl)], and all chlorine (in the two DAZZLER assumptions) reacted to either Cl_2 (1648 moles) or HCl (3295 moles).

** Negative values indicate consumption of atmospheric O_2 after all the oxygen in the carbon-bearing items (propellant+explosives+motor parts) is consumed.

Table B3. Data summary—comparison of computed and measured bulk gas species concentrations in the test chamber at the end of each burn *

Gas Species	SUNSPOT, % Vol Expect	Meas'd	± %V	THUNDERBIRD, % Vol Expect	Meas'd	± %V	DAZZLER, % Vol Expect	Meas'd	± %V
Nitrogen	75.42	75.63	0.10	73.20	75.13	0.5	76.45	77.10	0.1
Oxygen	13.45	13.14	0.10	6.75	4.48	0.5	16.22	16.20	0.1
Carbon Dioxide	10.01	9.95	0.10	19.00	19.01	0.5	4.10	4.17	0.1
Argon	0.88	0.87	0.02	0.84	0.85	0.02	0.90	0.90	0.02
Krypton	0.23	0.22	0.01	0.20	0.20	0.01	0.218	0.204	0.002
Neon							0.238	0.206	0.0006
Hydrogen Chloride							1.88	--	
		ppmv	±ppmv		ppmv	±ppmv		ppmv	±ppmv
Carbon Monoxide		682	42		1692	100		234	42
Hydrogen		64	6		299	20		497	6
Nitrogen oxides: NOx		1169	50		1324	50		1425	50
NO		1017	50		1164	50		1292	50
NO₂, by difference		152	50		159	50		133	
Methane		50	10		70	20		<10	10
Net Test Weight, lb°°		1606			3212			1334	

* *Expect* assumes only CO_2, N_2, H_2O, metal oxides and HCl (in DAZZLER) are formed and added to an initial atmosphere at 20°C, 60% relative humidity, and a pressure of 0.88 atmosphere with a volume of 4644 m^3; note that initial CO_2 concentration was 200ppmv for SUNSPOT and THUNDERBIRD and 325ppmv for DAZZLER

* *Meas'd* values are obtained by extrapolating time-resolved gas concentration measurements back to test initiation time plus 60s (i.e., T=60s). These values are normalized to 100% on a water-free basis. Data from the sampling port on the tunnel back were used for obtaining the SUNSPOT and DAZZLER measurements. For THUNDERBIRD, the data shown represent an average from two measurements taken at the back and invert ports at 5 and 9 minutes, respectively. For this reason, it is assumed that the SUNSPOT and DAZZLER measurements represent maximum values, whereas the THUNDERBIRD measurements are an average.

* ± %V indicates the precision of the measured values except for values of NO₂, by difference and DAZZLER Kr and Ne. The uncertainty on NO₂ is the square root of the squared errors for NOx and NO. The uncertainty on the DAZZLER Kr and Ne values is the uncertainty on the intercept of a linear regression data fit.

°° Initial weight of carbon bearing materials in the test

46

The gas species concentrations in Table B3 were measured in each test by extracting samples from the test chamber. These samples, composed of combustion product gases mixed with ambient air and tracer gas, were extracted from the test chamber using two sampling ports. One port was at the invert, and the second one was located on the back of the chamber. Stainless steel sampling lines from each port were routed out of the test chamber and over a distance of roughly 300 m to a pumping station located on the apron of the X-tunnel complex. The combustion gases were analyzed in real time by standard analytical instruments located near the pumping station. The transit time of the gases between the test chamber and the analysis station was roughly 120 s.

Since the gases in the test chamber tend to become stratified (i.e., hotter gases collecting near the tunnel back), we instituted a general procedure focused on analyzing the gas stream from the port on the chamber back. In general, this gas stream was analyzed for roughly 30 minutes before switching to the invert port for roughly 10 minutes before returning to the port at the chamber back. The one exception to this procedure occurred in the THUNDERBIRD test where we found the sampling port on the back of the chamber was non-operable roughly 7 minutes after the test was initiated. This failure was probably caused by high debris loading in the combustion cloud that clogged the sample port inlet filter. After the back sampling port became clogged, the invert port was used exclusively for gas sampling in THUNDERBIRD.

The histories of the O_2 and CO_2 concentrations during the first 20 minutes after initiation of the SUNSPOT test as given in Figure B1 are examples of the data obtained from these measurements. Similarly, the time histories of the NOx species for 250 minutes in SUNSPOT are shown in Figure B2. It is evident from Figure B1 that, once the propellant burn is completed, the concentrations of the relatively stable O_2 and CO_2 gas species are essentially constant. It can also be seen that the measured concentrations of these species depend somewhat on sampling location. The full data record for the CO_2 concentration history in SUNSPOT is given in Figure B3. This record shows a gradual decrease in CO_2 concentration over the 3-4 hour sampling period for the test. In contrast, we see in Figure B2 over a comparable time scale that the concentration histories of the highly reactive NOx species in the combustion cloud are characterized by:

strong peaks followed by rapid decreases, and

long-term molecular stratification in the chamber.

The occurrence of the concentration peaks in Figure B2 correlates well with the end of the propellant burn. The stratification is evident from the persistent factor of 2 difference in the NOx gas concentrations measured at the invert and back sampling locations. However, in the interest of reporting conservative data in Table B3, we list only the highest values of the measured nitrogen oxide concentrations at the end of each test burn (i.e., derived from samples taken at the chamber back).

47

A summary of the carbon burn efficiency (overall carbon balance) computed from the test results is given in Table B4. These results suggest that the conversion of the carbon materials inventory in each test to carbon-containing gas species is complete. In the NIKE rocket motor burn tests, the CO_2 values are slightly greater than 100%, but within the 1-sigma uncertainty of the result. In contrast, the data from DAZZLER suggest the presence of excess CO_2 in the test chamber. A possible explanation for this anomaly is that some of the CO_2 absorbed in the chamber walls from previous tests may have been released in DAZZLER due to the elevated temperatures and the high concentration of acid gases in that test. Note also that less than 1% of the carbon was converted to CO and CH_4 in every test. This observation suggests that the combustion process in the test chamber proceeded very nearly to completion, which is consistent with the assumptions used above in calculating the expected gas species concentrations shown in Table B3.

Table B4. Carbon balance

	SUNSPOT		THUNDERBIRD		DAZZLER	
	% Total C	±%TC	% Total C	±%TC	% Total C	±%TC
CO2	103.89	3.85	101.89	5.75	108.85	2.80
CO	0.71	0.05	0.91	0.07	0.62	0.11
CH4	0.05	0.01	0.04	0.01		
Gas sum	105	4	103	6	109	3

% Total C =100 x (moles carbon in gas product) / (initial total moles carbon in the test materials)
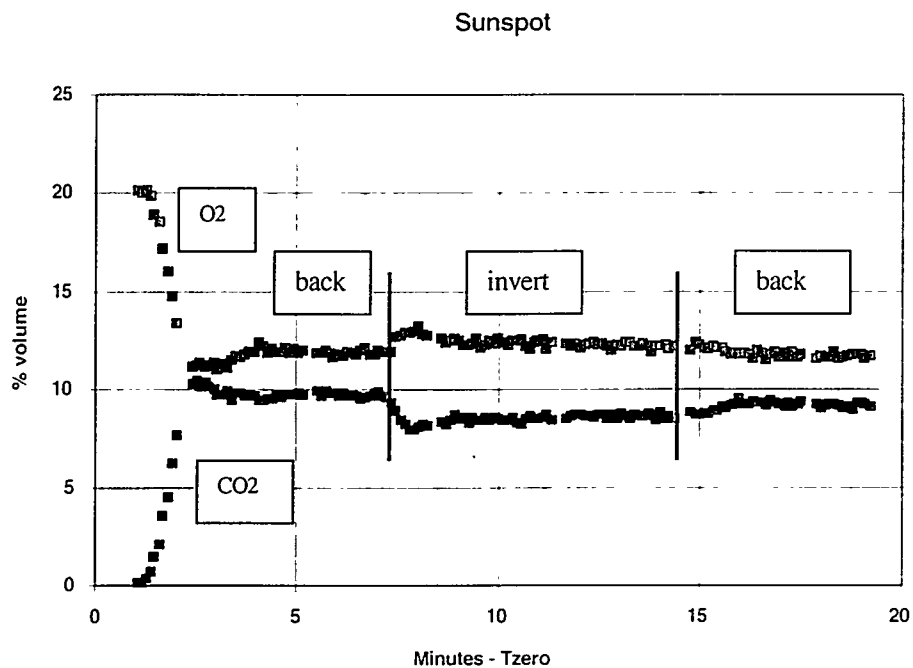
Figure B1. Early-time variation of O_2 and CO_2 gas concentrations in test chamber during SUNSPOT test. Samples extracted from chamber back and invert as indicated.
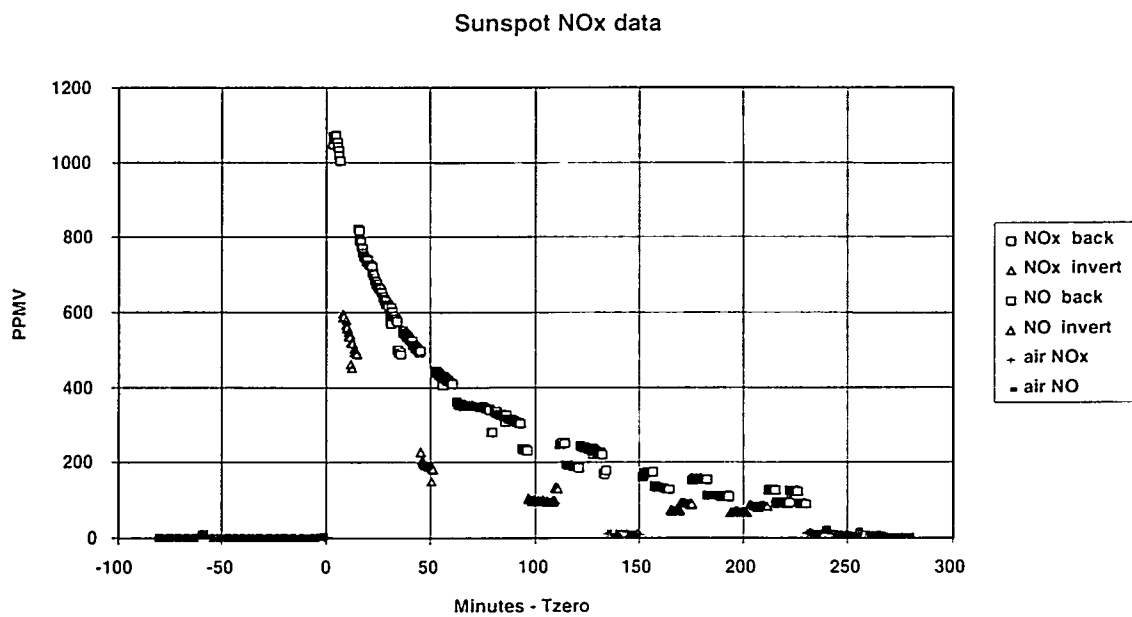
Figure B2. Variation of NOx gas concentrations in test chamber during SUNSPOT test (samples taken from invert and back).

49
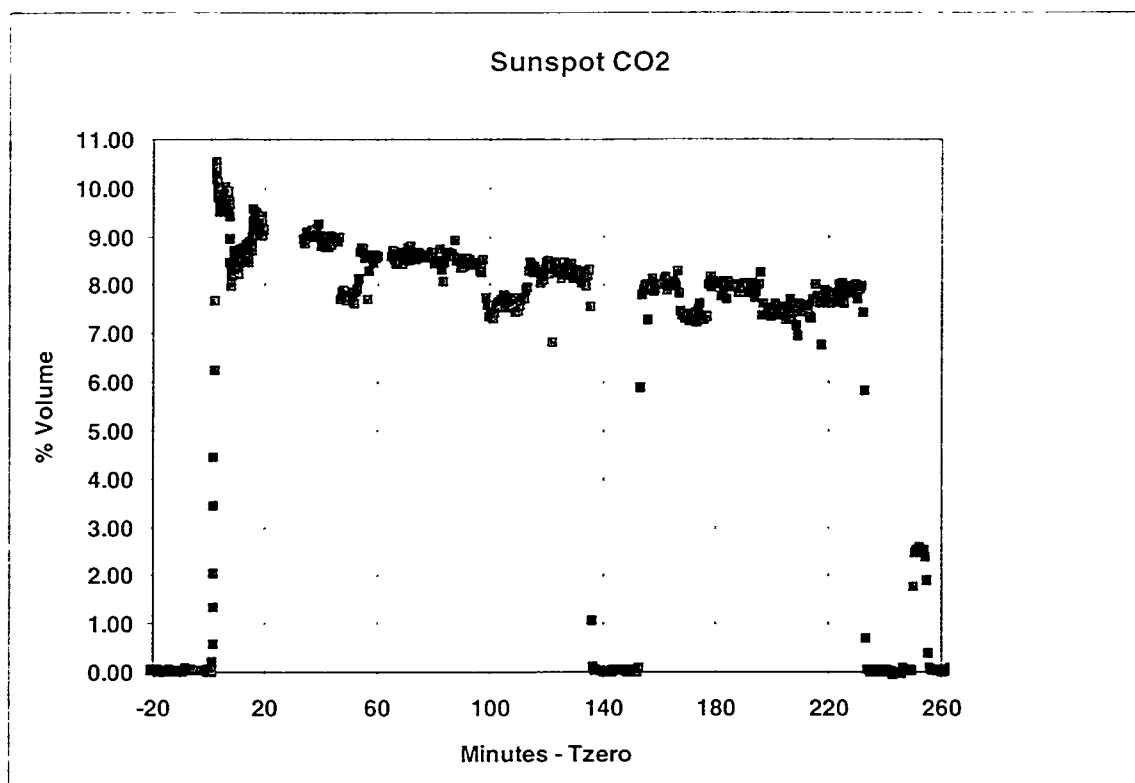
Figure B3. Complete history of CO_2 concentration in SUNSPOT.

APPENDIX C

Real-Time and Time-Averaged Aerosol Analyses—LANL

The LAASS impactor and streaker aerosol measurement elements provided data on the evolution, size distribution and composition of the particulate in the combustion cloud after each rocket motor burn test. Time-resolved elemental analyses (i.e., PIXE results) from the streaker are summarized in Tables C1-C6. Data from SUNSPOT are given in Tables C1 and C2 for the total (<10 μm) and fine (<2.5 μm) aerosol fractions, respectively. The same aerosol size distinction is used for streaker data obtained from the THUNDERBIRD (Tables C3 and C4) and DAZZLER (Tables C5 and C6) tests. These data also give us an indication of the evolution of the total aerosol concentrations in the test chamber. The sums of the elemental concentrations at each sampling time for the two aerosol size categories provide this information. These results for the SUNSPOT, THUNDERBIRD and DAZZLER tests are presented in Figures C1-C3, respectively. The rapid changes in the elemental concentration data shown in Figure C3 are physically unrealistic and may be the result of a measurement error. Additional analyses are required to resolve this issue.

The time histories of the aerosol size distributions obtained from the LAASS impactor measurements are reported in Figures C4-C6 for the SUNSPOT, THUNDERBIRD and DAZZLER tests, respectively. Figure C4 shows the aerosol size distribution obtained from the impactor 27 minutes after initiation of the motor burn in SUNSPOT. One of the impactor channels (1.2 - 2.5 μm) was inoperative during this test. In addition, because of an error in operating the flow controllers for the impactor, the impactor was not operated in an isokinetic condition for this sample. The aerosol concentration data therefore represent a lower limit to the actual aerosol concentration. Figure C5 shows the impactor data obtained for the first two sampling times in the THUNDERBIRD test. Note that dynamic processes in the test chamber (e.g., particle coagulation and thermally driven turbulence) likely affect the aerosol concentrations reported here. Thus, even though the quantities of propellant consumed in the SUNSPOT and THUNDERIRD tests differ by a factor of two, the aerosol concentration in a given bin size will not show a similar scale dependence. A more meaningful test-to-test comparison is the aerosol mass integrated over all sizes. Finally, Figure C6 shows impactor data for the first three sampling times in the DAZZLER test. Unlike the comparable data from SUNSPOT and THUNDERBIRD, the results in Figure C6 suggest a shift in aerosol size distribution from larger to smaller sizes over the three sampling times. This shift may reflect propellant differences in the tests (smaller aerosols showing less coagulation than in previous tests), or it may be associated with the differing sample delay times in each test. The decrease in aerosol concentration observed for latter samples is also consistent with the streaker results for DAZZLER.

Table C1. Total (<10 µm) Elemental Concentrations—(µg/m³) for SUNSPOT

Sample Time	(minutes):	26	39	62	79	101
Atomic Number	Element	Concentration				
		Sample 1	Sample 2	Sample 3	Sample 4	Sample 5
11	Na	0	0	0	0	0
12	Mg	0	0	0	0	0
13	Al	0	0	0	0	0
14	Si	3179.69	2176.42	2011.35	1583.43	1553.79
15	P	10372.5	7601.45	7956.44	5660.62	5794.44
16	S	0	0	0	1174.75	750.849
17	Cl	5759.18	5176.61	4804.79	2941.69	2905.63
18	Ar	0	0	0	0	0
19	K	992.051	779.297	812.712	535.771	532.807
20	Ca	3056.29	2218.89	1727.67	1292.55	1314.19
21	Sc	0	0	0	0	0
22	Ti	221.569	79.332	49.9231	87.9063	47.9999
23	V	0	0	0	0	0
24	Cr	42.2303	18.7993	40.884	17.413	15.4818
25	Mn	0	3.91852	0	0	0
26	Fe	2378.36	1742.1	1835.05	1324.6	1358.26
27	Co	0	0	0	0	0
28	Ni	0	0	0	0	0
29	Cu	1185.41	875.857	916.886	668.552	685.941
30	Zn	1198.15	884.191	926.341	680.893	685.941
31	Ga	0	41.8296	18.6711	0	15.3856
32	Ge	0	0	0	0	0
33	As	289.121	191.198	153.696	190.878	158.023
34	Se	8.26175	37.2299	11.5873	21.3716	9.3756
35	Br	170.444	134.408	176.053	117.155	123.566
48	Cd	2600.33	1915.99	2079.46	1792.58	1708.44
49	In	0	0	0	0	0
50	Sn	0	0	0	0	0
51	Sb	37622.6	27822.3	30170.2	21259.4	21900.4
82	Pb	118774	89541	96961.3	69804.1	71719.3

Table C2. Fine (< 2.5 μm) Elemental Concentrations—(μg/m^3) for SUNSPOT

Sample Time (minutes):		26	39	62	79	101
Atomic Number	Element	Concentration				
		Sample 1	Sample 2	Sample 3	Sample 4	Sample 5
11	Na	0	0	0	0	0
12	Mg	0	0	0	0	0
13	Al	0	0	0	0	0
14	Si	2102.7	1410.35	1173.95	947.977	893.487
15	P	9023.01	6402.65	5320.85	4030.71	3966.6
16	S	0	0	0	1174.75	750.849
17	Cl	5304.83	4623.69	3421.69	2342.3	2228.51
18	Ar	0	0	0	0	0
19	K	769.28	611.417	512.052	361.401	344.573
20	Ca	2226.91	1667.57	1065.77	864.639	860.632
21	Sc	0	0	0	0	0
22	Ti	133.582	0	0	22.1168	0
23	V	0	0	0	0	0
24	Cr	42.2303	15.7061	32.8547	9.05507	10.6577
25	Mn	0	3.91852	0	0	0
26	Fe	1895.95	1338.23	1153.92	851.817	846.208
27	Co	0	0	0	0	0
28	Ni	0	0	0	0	0
29	Cu	967.209	687.544	579.364	432.72	431.919
30	Zn	954.388	669.113	570.549	426.309	404.673
31	Ga	0	41.8296	18.6711	0	15.3856
32	Ge	0	0	0	0	0
33	As	262.036	130.617	83.3387	73.8829	70.5975
34	Se	0	25.8029	0	8.81467	9.3756
35	Br	138.23	108.741	110.023	78.8512	84.0599
48	Cd	2314.25	1617.09	1370.28	1268.51	1123.47
49	In	0	0	0	0	0
50	Sn	0	0	0	0	0
51	Sb	32534.1	23198.6	19889.1	14680.4	14696.5
82	Pb	102651	74363.7	63385.5	46958.1	45996.5

Table C3. Total (<10 μm) Elemental Concentrations—(μg/m³) for THUNDERBIRD

Sample Time	(minutes):	19	32	43	54	63
Atomic Number	Element			Concentration		
		Sample 1	Sample 2	Sample 3	Sample 4	Sample 5
14	Si	5755.18	5418.62	3365.6	3197.32	2452.08
15	P	9644.85	7712.03	5577.28	5067.63	4178.15
16	S	12563.3	12659.5	8173.6	8216.87	5288.8
17	Cl	5806.62	4086.8	3711.78	3192.51	3024.23
18	Ar	0	0	0	0	0
19	K	8308.22	6740.82	4740.69	4327.2	3557.92
20	Ca	5158.98	3726.2	2966.54	2658.82	1971.28
21	Sc	0	0	0	0	0
22	Ti	376.947	337.522	228.861	197.128	204.34
23	V	12.9335	0	0	0	13.7509
24	Cr	113.661	75.1971	40.3872	67.312	55.6766
25	Mn	53.3688	0	0	0	0
26	Fe	4870.5	3428.1	2639.59	2283.8	2149.18
27	Co	0	0	0	0	0
28	Ni	0	0	0	0	0
29	Cu	1485.19	1089.49	799.09	716.873	670.716
30	Zn	1941.95	1417.88	1064.97	945.253	840.438
35	Br	240.833	183.329	135.441	127.316	116.45
48	Cd	3405.03	2915.09	1716.94	1822.23	1591.45
49	In	0	0	0	0	0
50	Sn	0	0	0	0	0
51	Sb	29362.5	21549.5	15741.4	13875.9	13048.9
82	Pb	123325	91159.7	68129.4	60436.6	56061.3

Table C4. Fine (< 2.5 µm) Elemental Concentrations—(µg/m^3) for THUNDERBIRD

Sample Time	(minutes):	19	32	43	54	63
Atomic Number	Element			Concentration		
		Sample 1	Sample 2	Sample 3	Sample 4	Sample 5
14	Si	4904.16	4707.03	2812.68	2456.89	1682.8
15	P	8558.24	6635.04	4399.32	3682.93	2841.53
16	S	11202.6	11106.5	7356.24	6538.88	3706.97
17	Cl	5481.12	3596.38	2875.18	2379.96	2211.68
18	Ar	0	0	0	0	0
19	K	7500.48	5961.92	3923.33	3312.71	2519.39
20	Ca	4519.52	3178.09	2456.89	2072.25	1394.32
21	Sc	0	0	0	0	0
22	Ti	272.614	260.594	169.242	129.816	115.873
23	V	0	0	0	0	0
24	Cr	100.968	62.504	40.3872	47.503	37.262
25	Mn	53.3688	0	0	0	0
26	Fe	4057.95	2788.64	1947.24	1572.22	1394.32
27	Co	0	0	0	0	0
28	Ni	0	0	0	0	0
29	Cu	1327.01	932.752	620.232	524.072	466.857
30	Zn	1682.8	1177.96	793.32	663.504	548.112
35	Br	205.302	154.818	94.7176	88.948	73.0816
48	Cd	3048.27	2548.24	1346.24	1317.39	1081.8
49	In	0	0	0	0	0
50	Sn	0	0	0	0	0
51	Sb	26155.5	18558.9	12020	10000.6	8894.8
82	Pb	107218	75966.4	50964.8	42118.1	36781.2

Table C5. Total (< 10 µm) Elemental Concentrations—(µg/m^3) for DAZZLER

Sample Time (minutes):		10	22	32	43	52	62	72	82
Atomic Number	Element					Concentration			
		Sample 1	Sample 2	Sample 3	Sample 4	Sample 5	Sample 6	Sample 7	Sample 8
11	Na	0	0	0	0	0	0	0	0
12	Mg	1877.52	2769.41	110.344	1177.96	805.34	1233.25	935.156	1012.08
13	Al	106690	113589	11419	67864.9	39666	35555.2	46829.9	47286.7
14	Si	0	158.424	0	0	0	245.208	0	0
15	P	0	0	0	0	0	0	0	0
16	S	644.272	926.982	0	399.064	153.616	163.472	310.116	147.365
17	Cl	668.072	1022.9	123.085	564.219	428.393	321.174	426.71	460.126
18	Ar	0	0	0	0	0	0	0	0
19	K	358.196	351.946	13.0537	205.542	104.814	99.2852	78.13	123.806
20	Ca	410.363	356.994	57.72	226.938	114.671	124.046	80.2936	116.594
21	Sc	0	0	0	0	0	0	0	0
22	Ti	66.4706	69.7641	11.669	53.3688	20.5542	26.6844	12.02	20.3378
23	V	0	0	0	0	0	0	0	0
24	Cr	210.614	199.556	35.8196	135.562	65.4369	60.8933	36.685	64.908
25	Mn	29.0884	0	0	19.9292	6.611	0	0	17.6934
26	Fe	1662.85	1230.37	169.722	674.562	360.36	330.31	189.676	364.206
27	Co	0	0	0	0	0	0	0	0
28	Ni	0	0	1.47125	1.51692	0	0	0	0
29	Cu	1791.7	1658.28	176.454	965.687	492.339	442.817	260.594	495.945
30	Zn	126.955	120.368	18.4868	71.0622	38.4159	34.1368	19.6407	37.9111
31	Ga	12.6931	11.1786	0	1.45923	0	0	0	4.30316
32	Ge	0	0	0	0	0	0	0	0
33	As	0	0	0	23.415	0	0	0	0
34	Se	0	0	0	0	0	0	0	0
35	Br	0	0	0	0.723604	3.87044	2.42804	0	1.61789
51	Sb	113.95	323.338	0	267.325	144	82.938	69.4756	157.222
82	Pb	1426.53	1361.14	171.165	764.712	416.132	372.62	226.938	432.239

56

Table C6. Fine (< 2.5 μm) Elemental Concentrations—(μg/m^3) for DAZZLER

| Sample Time (minutes):		10	22	32	43	52	62	72	82
Atomic Number	Element					Concentration			
		Sample 1	Sample 2	Sample 3	Sample 4	Sample 5	Sample 6	Sample 7	Sample 8
11	Na	0	0	0	0	0	0	0	0
12	Mg	1334.22	1807.81	110.344	668.312	425.508	372.62	480.8	507.244
13	Al	85582.4	93275.2	6611	49522.4	21563.9	22020.6	30050	25482.4
14	Si	0	0	0	0	0	0	0	0
15	P	0	0	0	0	0	0	0	0
16	S	644.272	726.008	0	399.064	153.616	163.472	310.116	147.365
17	Cl	500.032	798.128	48.08	377.428	191.839	174.771	228.861	188.474
18	Ar	0	0	0	0	0	0	0	0
19	K	312.52	300.5	0	175.011	65.6292	68.514	42.3104	76.928
20	Ca	365.408	312.52	34.3772	185.108	74.7644	87.746	38.7044	65.8696
21	Sc	0	0	0	0	0	0	0	0
22	Ti	57.9364	63.706	9.47176	47.3588	14.7125	20.6744	6.58696	13.4864
23	V	0	0	0	0	0	0	0	0
24	Cr	189.195	179.819	26.9248	115.152	46.6376	42.7912	18.2704	40.3872
25	Mn	29.0884	0	0	19.9292	6.611	0	0	17.6934
26	Fe	1526.54	1110.65	131.499	569.748	257.228	233.428	93.5156	227.418
27	Co	0	0	0	0	0	0	0	0
28	Ni	0	0	0	0	0	0	0	0
29	Cu	1629.91	1502.5	137.028	831.784	355.792	319.732	131.98	317.328
30	Zn	115.392	109.622	14.5923	60.1	28.3672	24.5208	9.95256	24.7612
31	Ga	12.6931	11.1786	0	0	0	0	0	2.74056
32	Ge	0	0	0	0	0	0	0	0
33	As	0	0	0	23.415	0	0	0	0
34	Se	0	0	0	0	0	0	0	0
35	Br	0	0	0	0	3.87044	2.42804	0	1.61789
51	Sb	79.5724	281.268	0	233.669	93.9964	40.3872	25.7228	102.17
82	Pb	1281.33	1221.23	135.345	641.868	288.48	259.632	108.42	266.844
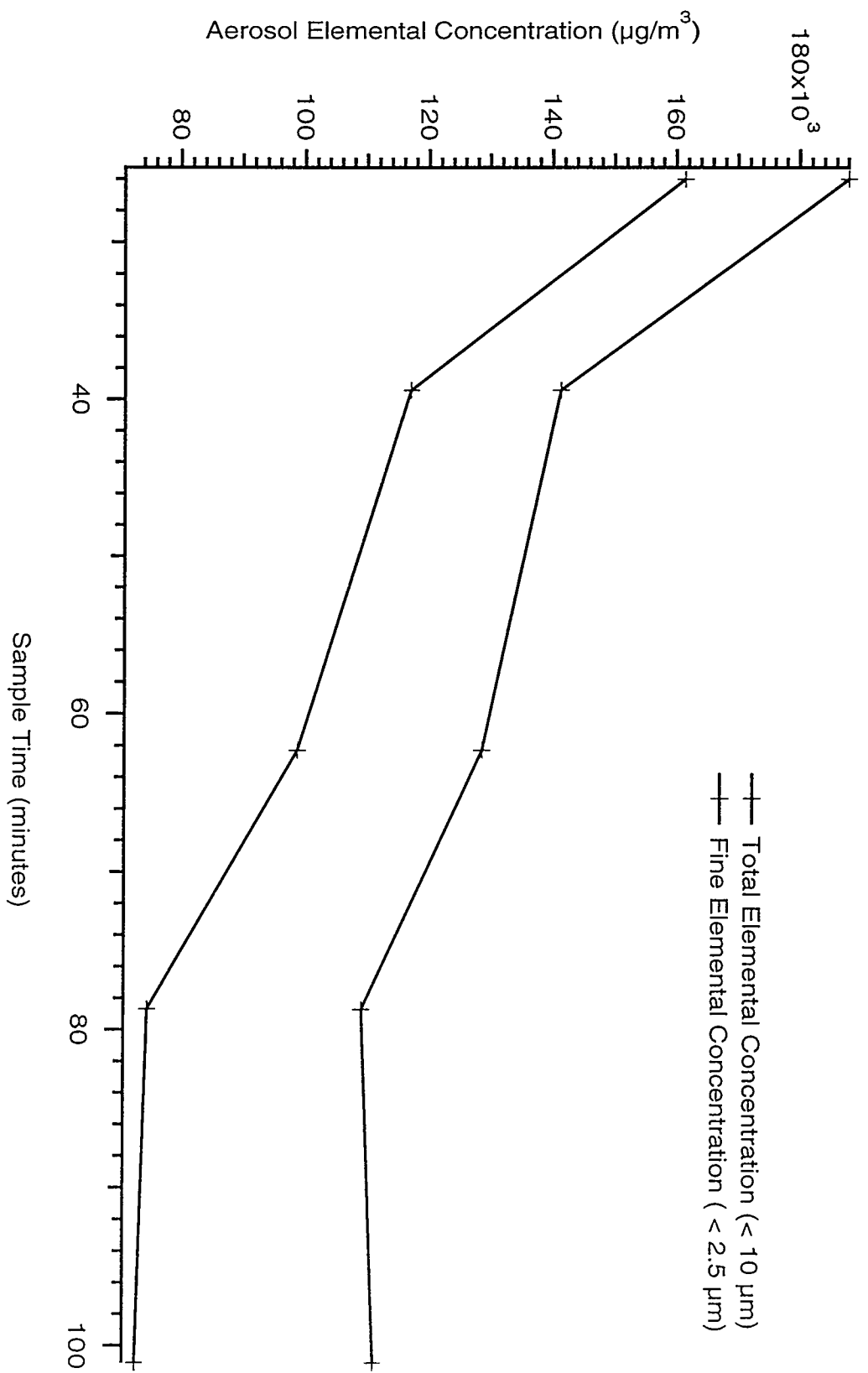
Figure C1. Summary of LAASS streaker elemental composition data from SUNSPOT
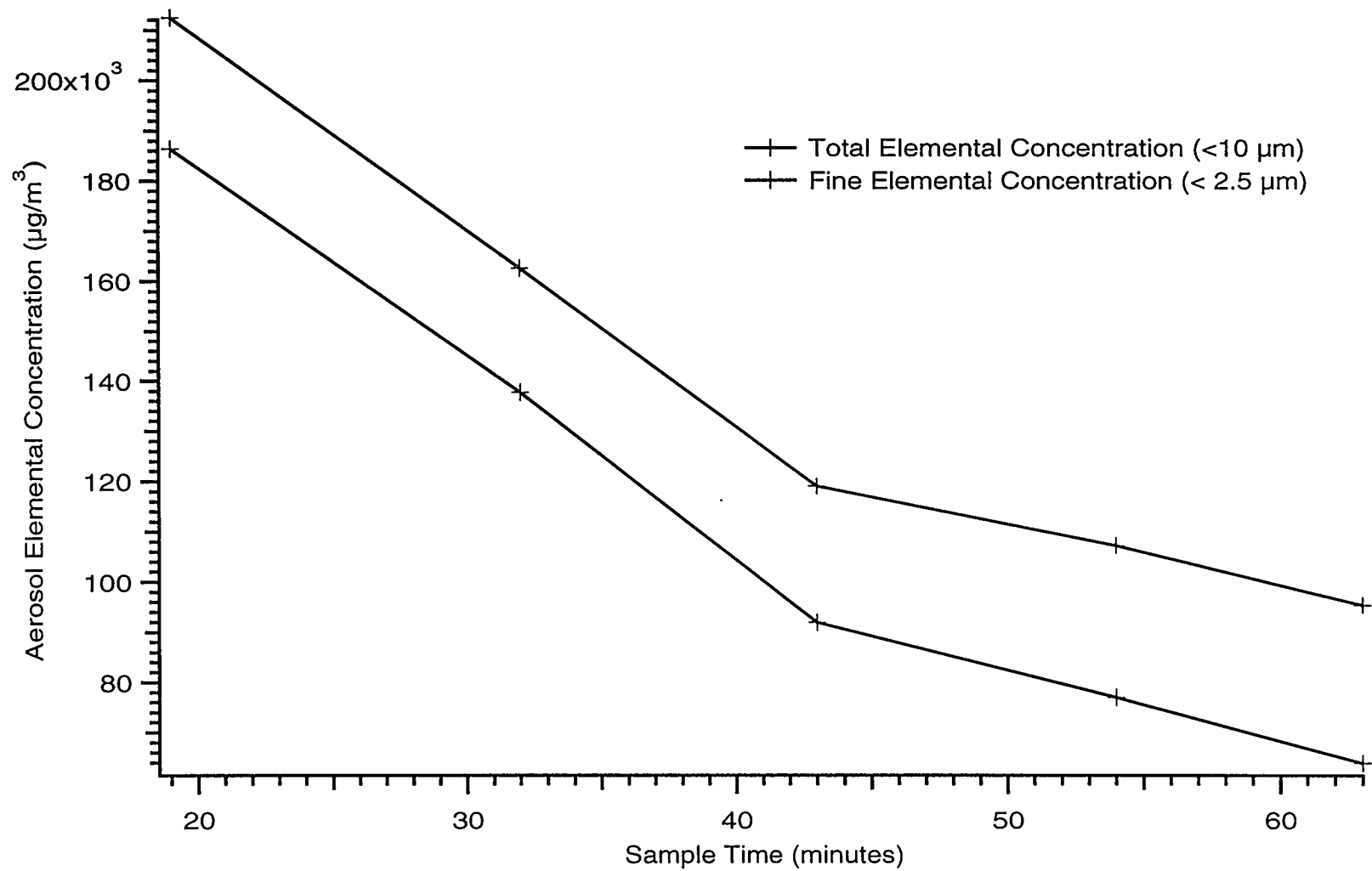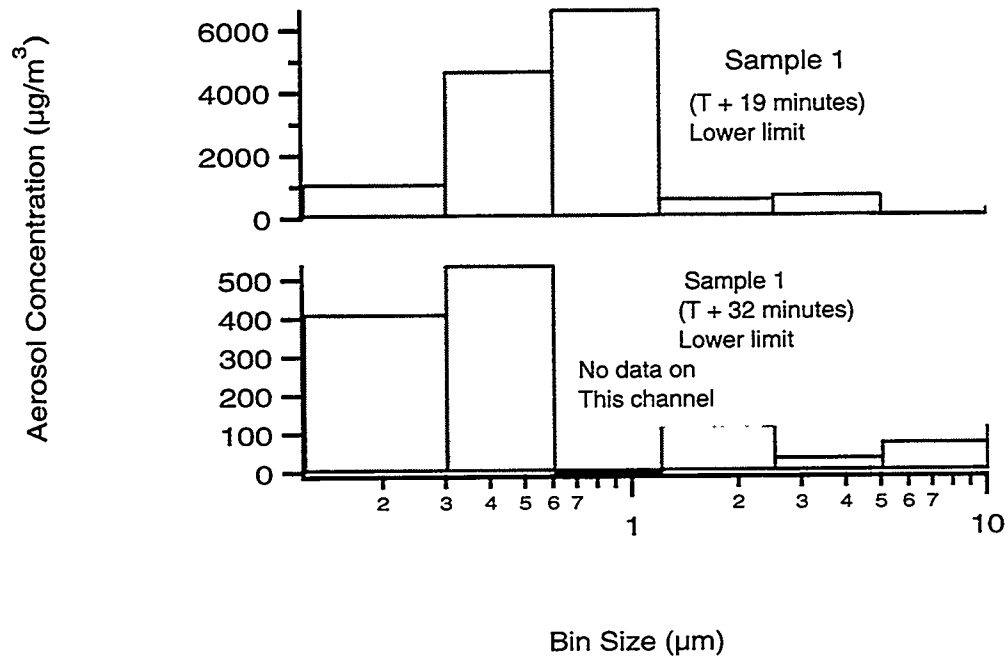
Figure C2. Summary of LAASS streaker elemental composition data from THUNDERBIRD
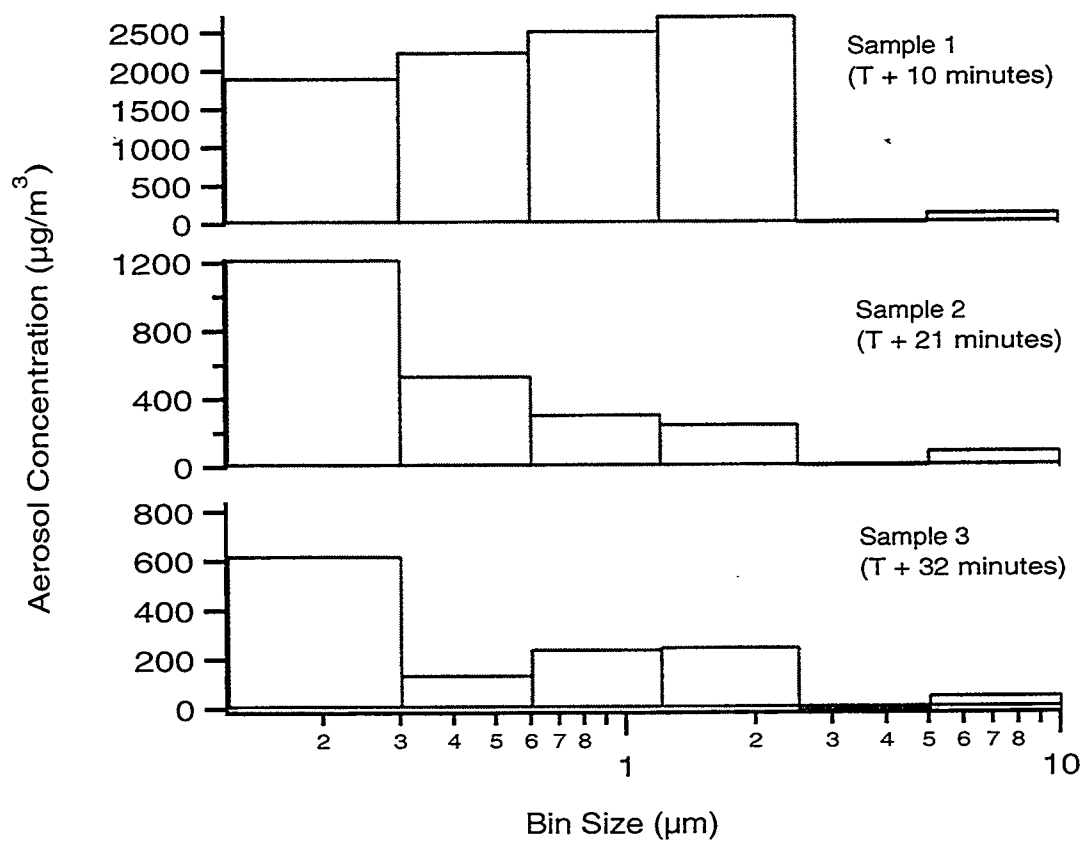
59
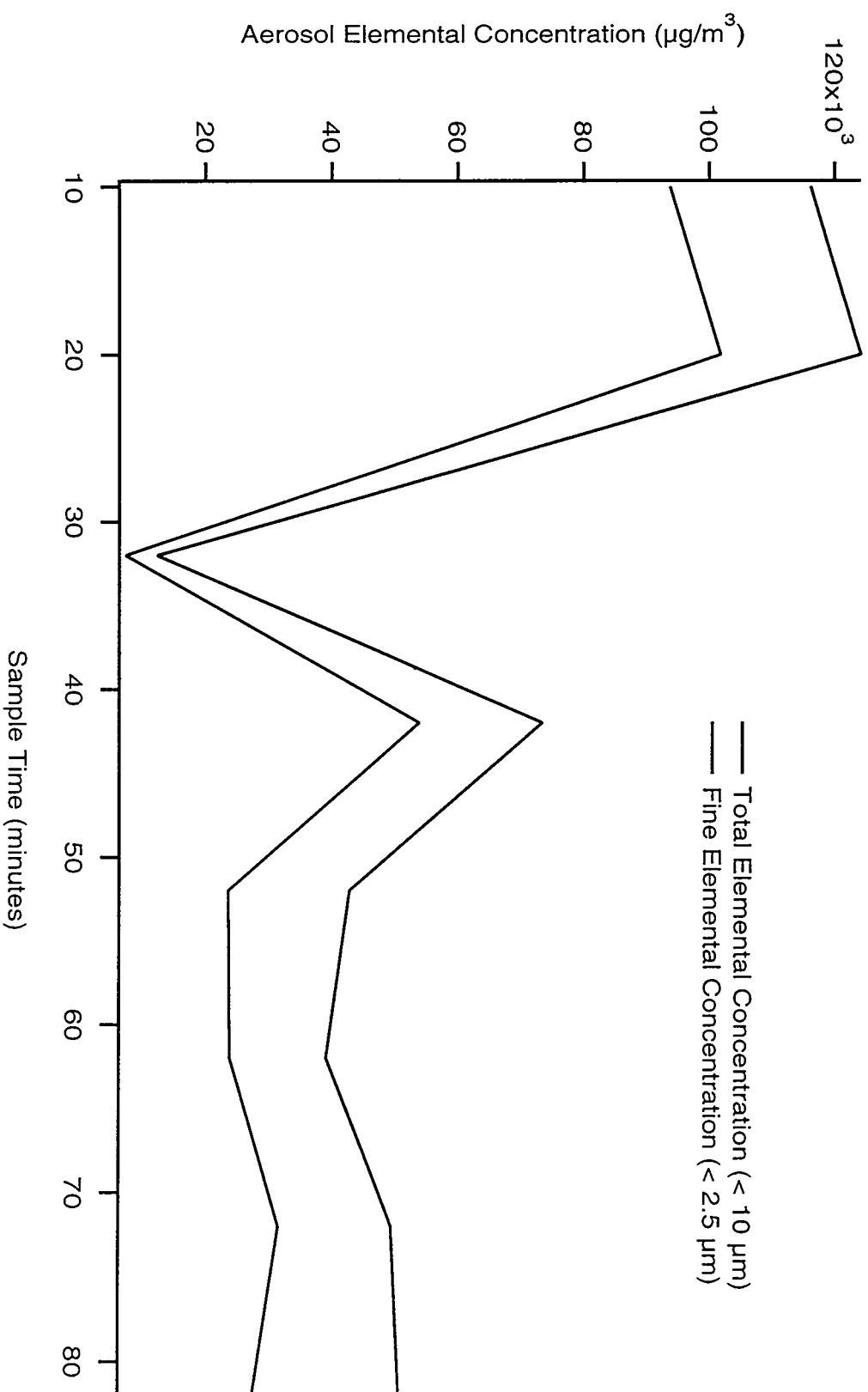
Figure C3. Summary of LAASS streaker elemental composition data from DAZZLER

60
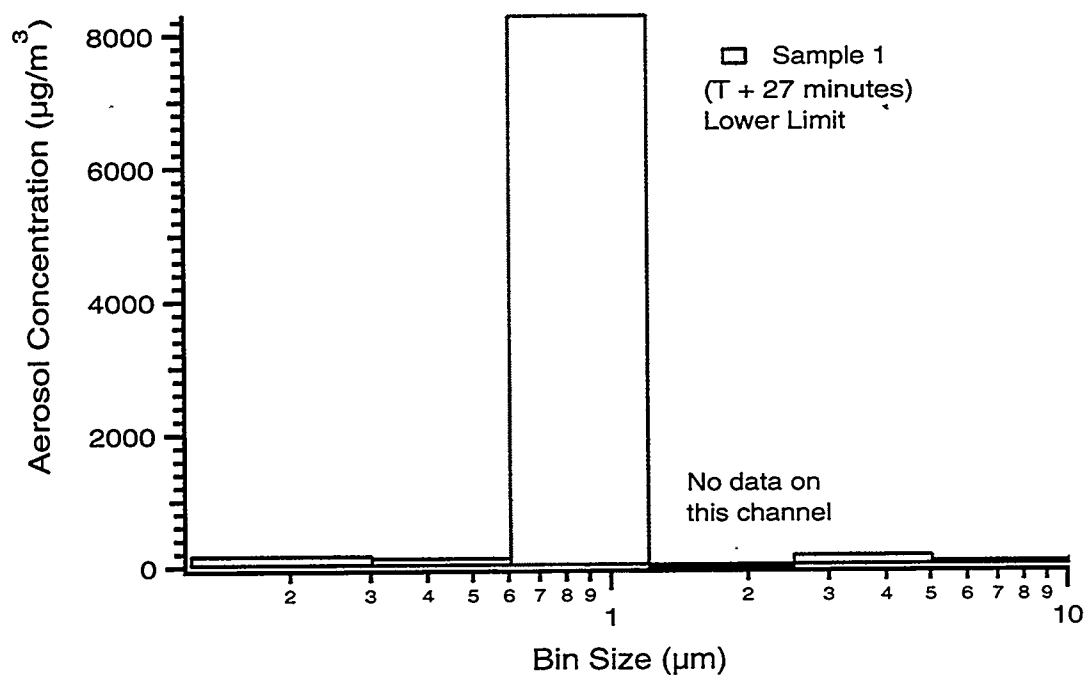
Figure C4. Summary of LAASS impactor data from SUNSPOT

**Figure C5.** Summary of LAASS impactor data from THUNDERBIRD

61

Figure C6. Summary of LAASS impactor data from DAZZLER

APPENDIX D

Real-Time Gas Species Analyses Using FTIR—LANL

The FTIR diagnostic was implemented primarily to obtain time-resolved measurements of HCl gas concentrations in DAZZLER. Nevertheless, it was available to analyze gas samples extracted from the THUNDERBIRD test. The FTIR was therefore used in this test to establish operational procedures for it in X-tunnel, rather than for collecting critical data. Only a single FTIR spectrum was obtained in THUNDERBIRD because the substantial particulate loading in this test clogged an in-line, small-particulate filter located in the sampling line. This interruption occurred soon after the first sample was extracted from the test chamber. In addition, it appears that a water-based aerosol entered the sample cell despite the precaution of using a heated sample line.

To quantify the results for CO_2, CO and H_2O concentrations observed in this first scan, the background scan obtained prior to executing the THUNDERBIRD test was used as a reference to obtain the absorbance spectrum shown in Figure D1. This spectrum is a function of the concentrations of the gas species detected. We can obtain good estimates of these concentrations either by calculating the spectrum from known databases parameters or by adjusting tabulated spectra from available quantitative databases. The later was done here, using the QASOFT[1] database to quantify the concentrations of CO, CO_2 and H_2O in the sample at 0.2 %, 10 %, and 10 %, respectively. The spectra used for these analyses are shown in Figure D2.
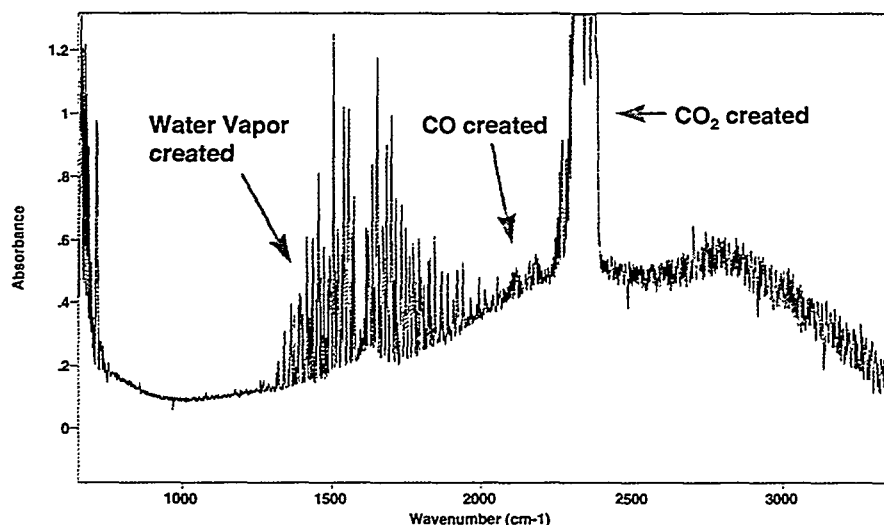
Figure D1. Absorbance spectra from first FTIR scan in THUNDERBIRD (sample taken at test initiation time + 19 minutes)

---

[1] P. L. Hanst and S. T.Hanst, "Infrared Spectra for the Quantitative Analysis of Gases", Infrared Analysis, Inc., Anaheim, CA
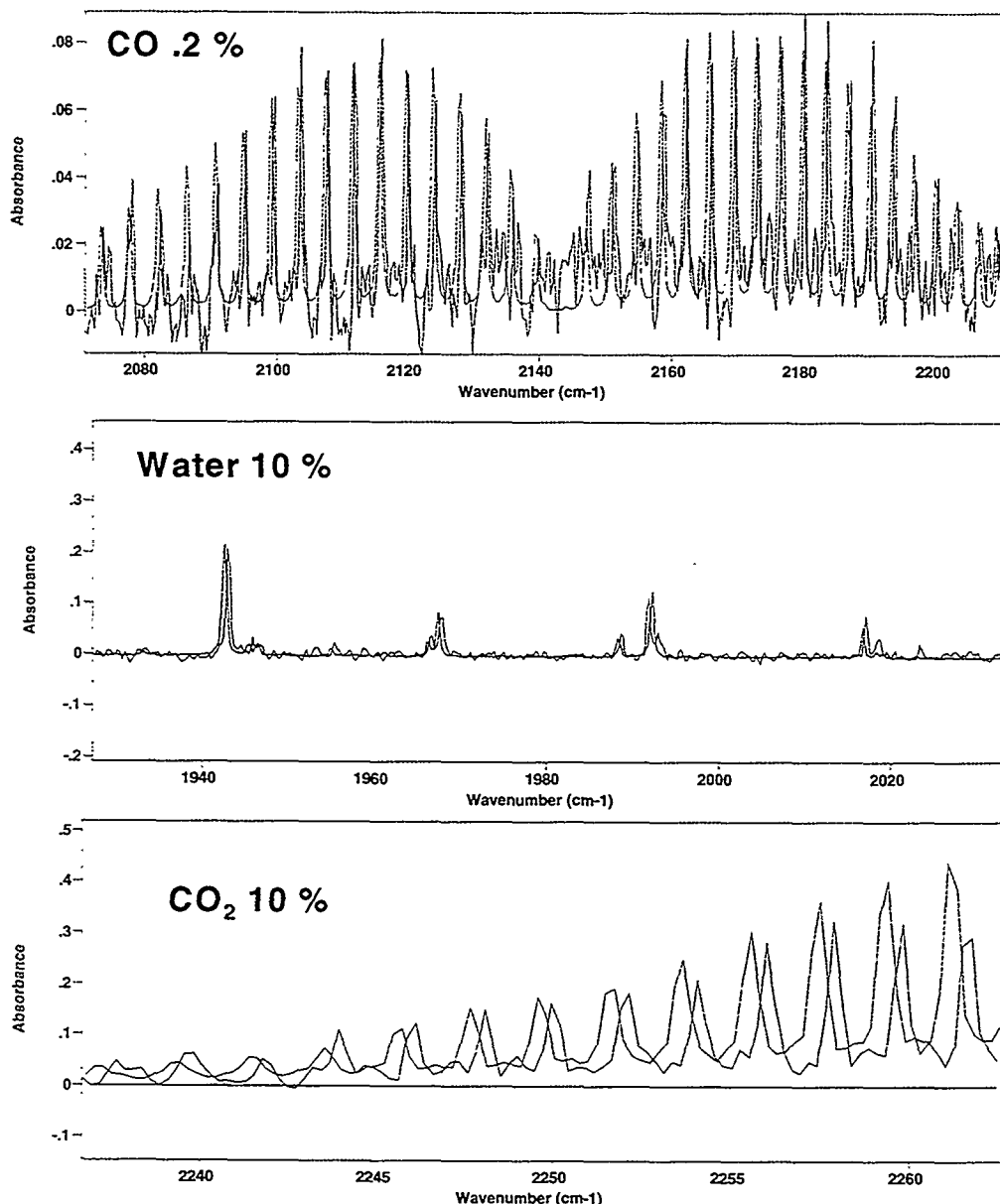
Figure D2. Comparison between measured and simulated absorption features for water, CO and. CO_2. Simulated spectra are derived from the QASOFT database. Estimated concentrations are indicated for each simulation.

Thirteen FTIR spectra were obtained using extracted samples from the DAZZLER test. This improved performance of the FTIR diagnostic (compared to the results in THUNDERBIRD) is related to changes in the sampling procedures implemented between the tests. In addition, a different combustion cloud aerosol size distribution in DAZZLER helped reduce particulate loading in the sampling line to the FTIR. However, no HCl peaks were observed in the thirteen spectra. Subsequent analysis of the FTIR diagnostic and comparison to QASOFT spectra suggest that an HCl concentration greater than 0.2 % should have been detectable by the instrument. The measurement of HCl concentration in

DAZZLER obtained by Radian International from post-test analyses of extracted samples was roughly 1.1%. Analyses of the FTIR spectra from DAZZLER shown in Figure D3 indicate upper limits of 0.5%, 0.1%, 0.1% and 0.05% for the concentrations of NO, NO_2, N_2O, and HCN, respectively.
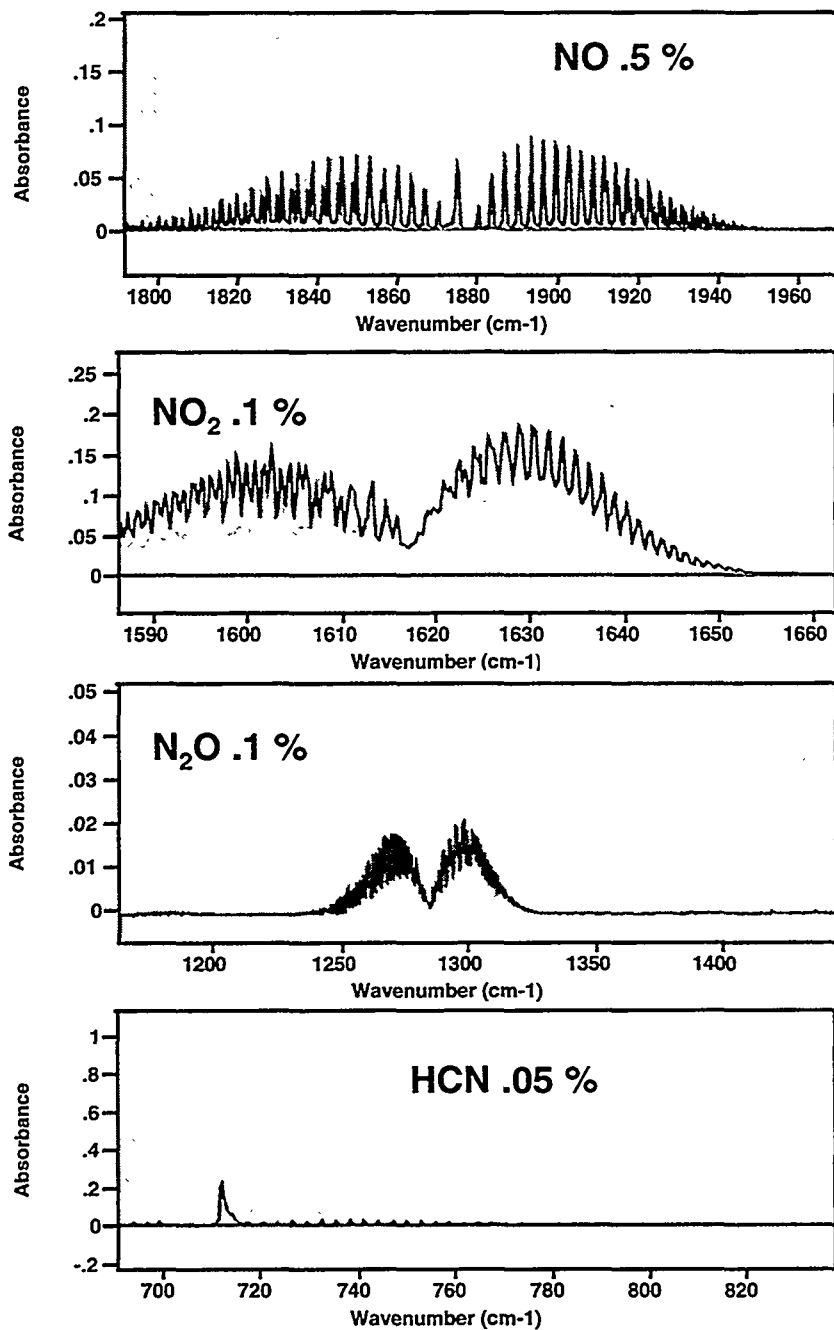
Figure D3. Representative spectra from DAZZLER (light background) compared with simulated absorption features from the QASOFT database (dark foreground).

This page intentionally left blank

APPENDIX E

Post-test Metal Residue Analyses—UNLV

The results of the UNLV analyses of the coupon rinse samples obtained after each rocket motor burn test are summarized in Table E1. These analyses identified the concentrations of non-volatile metal residues that remained on large aluminum plate coupons after they were exposed to the combustion clouds in the test chamber. The mounting of the plates before a test, and the recovery of the rinse solution (a 50/50 mixture of distilled water and alcohol) after a test, were the responsibility of Radian International. Since the plates were fixed vertically in the chamber at a height of roughly 3m above the invert, we speculate that the residue sample obtained from them was fairly representative of the non-volatile combustion cloud components in each test. Note that no effort was made to recover volatile or semi-volatile compounds from these samples.

Table E1. Summary of metal concentrations (in ppb) found in coupon rinse solution obtained after each contained rocket motor burn test.

Element	SUNSPOT M /SD	THUNDERBIRD M /SD	DAZZLER M /SD
Be 9	ND	ND	ND
Al 27	721 15	5411 56	1475000 13030
Cr 52	2.80 0.11	21.2 0.2	642 3
Cr 53	12.7 2.3	39.3 1.4	668 2
Mn 55	87.0 1.5	85.5 1.5	2683 58
Ni 60	10.4 0.2	8.73 0.45	179 1
Ni 62	10.8 0.4	10.1 1	179 5
Cu 63	78.8 1.4	640 11	1969 34
Cu 65	78.1 2.2	627 10	1954 53
Zn 66	311 7	409 14	272 3

Table E1. (Contd.)

Element	SUNSPOT M /SD	THUNDERBIRD M /SD	DAZZLER M /SD
Zn 68	301 14	409 8	270 8
As 75	6.65 0.81	25.2 0.7	16 0.3
Se 77	38.5 7.4	93.2 3	85.5 1
Se 82	0.273 0.889	2.46 0.78	0.51 0.55
Cd 111	56.9 2.1	317 11	60.2 1.7
Cd 114	56.2 0.6	315 6	60.5 1.5
Ba 135	19.1 0.4	67.6 2.5	32.8 0.8
Ba 137	19.6 0.2	69.4 2	33 0.5
Pb 207	2424 33	24200 434	2472 22
Pb 208	2459 44	24140 415	2467 33
Sb 121	364 5	6574 110	807 5
Sb 123	360 3	6564 57	796 14

M - Mean
SD -Standard Deviation

APPENDIX F

In Situ Laser-Based Measurements of Gas Species Concentrations—SNL

The tunable diode laser gas species monitor (TDL) was used in two of the three contained rocket motor burn tests in X-tunnel: SUNSPOT and DAZZLER. The TDL monitors were not used in THUNDERBIRD because it was anticipated that the transient high air temperature and substantial number of particles generated in that test would be detrimental to this instrumentation.

In these tests, the sensitivity of the TDL instrumentation at both its invert and rib locations was limited by laser transmittance. During SUNSPOT, laser transmittances at the rib location slowly decreased after initially recovering from a prompt attenuation at test initiation time, T= 0. Nevertheless, the optical paths for both lasers in the rib were completely blocked by T= 2000 s. Laser transmittance in the invert sample volume during SUNSPOT was essentially zero by T = 40 s. During DAZZLER, the overall laser transmittances increased somewhat after the initial drop-off at T= 0; allowing some gas species concentration measurements to be made during this test. The time history of the laser transmittance in DAZZLER was qualitatively similar to that observed in the detonation test series.

The results of the TDL measurements in the rocket motor burn tests are summarized in Table F1. Molecular species measurements during SUNSPOT are sparse: CO_2 and H_2O signals were detected and analyzed, but the laser transmittance was very low so the signals were weak. Conversely, during DAZZLER, CO_2 concentration histories were obtained in both locations, and the H_2O concentration history was measured at the rib location. While the CO_2 signal in the invert was characterized by a low signal: noise ratio, the measurements indicate that molecular stratification was present in DAZZLER, in qualitative agreement with results obtained in the detonation tests.

The CO_2 concentration histories measured at the invert and rib locations in DAZZLER are presented in Figures F1 and F2, respectively. Both curves have been smoothed using a binomial smoothing algorithm. This was particularly necessary for the invert measurements because of low laser transmittance. The final CO_2 concentrations are nominally 4% in the invert, and 6% in the rib. Equilibrium calculations for DAZZLER yield a fully-mixed final CO_2 concentration of 3.6%, compared to the on-line LLNL/BN measured value (early time) of 4.2%. Even with the large uncertainty seen in Figs. F1 and F2, these data suggest that the CO_2 concentration at the rib location is substantially higher than in the invert, even long after the combustion process is complete.

Table F1. TDL measurement summary for rocket motor burn experiments

	SUNSPOT	THUNDERBIRD	DAZZLER
Execution date	5/14/97	5/28/97	6/11/97
Load	2 Nike Rocket Motors	4 Nike Rocket Motors	2 Hawk Rocket Motors
Species monitored	$HCN;CO; CO_2; H_2O$	Did not participate.	$CO; CO_2; H_2O$
Species detected	$CO_2; H_2O$	---	CO_2 and H_2O
CO concentration	---	---	---
CO_2 concentration, rib location	9% peak	---	6%
CO_2 concentration, invert location	---	---	4%
Fully mixed CO_2 concentration[1]	10.01%	19.00%	not available
H_2O concentration added, rib location	---	---	2.4%
H_2O concentration added, invert location	---	---	--
Fully mixed H_2O concentration, 75% initial relative humidity	7.23%	---	not available
Final Transmittance (rib)	0%	--	13%

Water concentration measurements were also obtained at the rib location in DAZZLER. Low transmittance prevented comparable measurements at the invert location. The results are shown in Figure F3. The pre-event water concentration in the chamber ambient air was estimated at 2.1%. The data in Figure F3 indicate that the total water concentration in the sealed chamber long after propellant combustion was completed was roughly 4.5%, corresponding to a water concentration increase of 2.4% from the combustion products. No other measurement of water concentration history was obtained in DAZZLER.
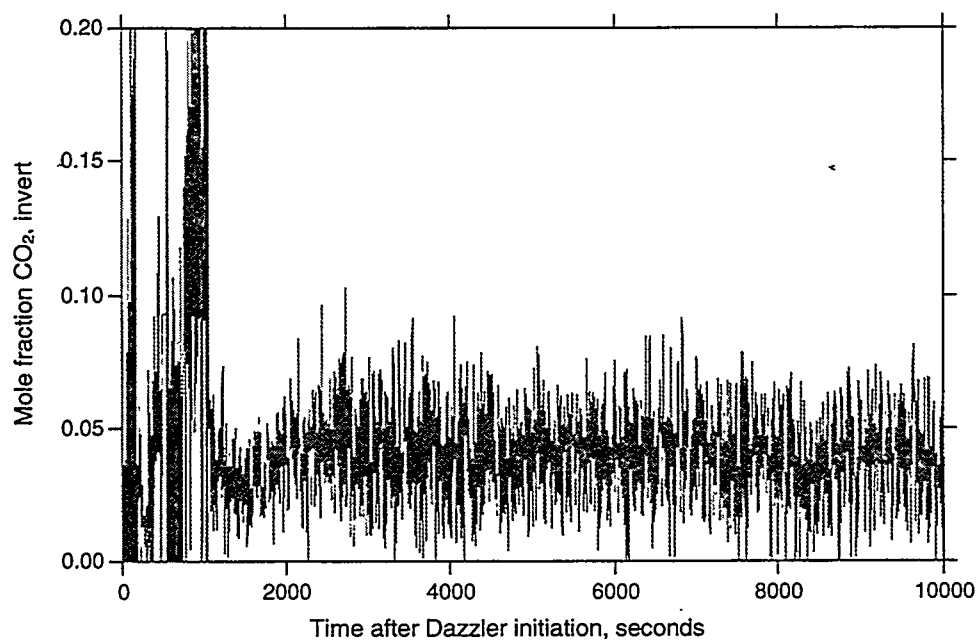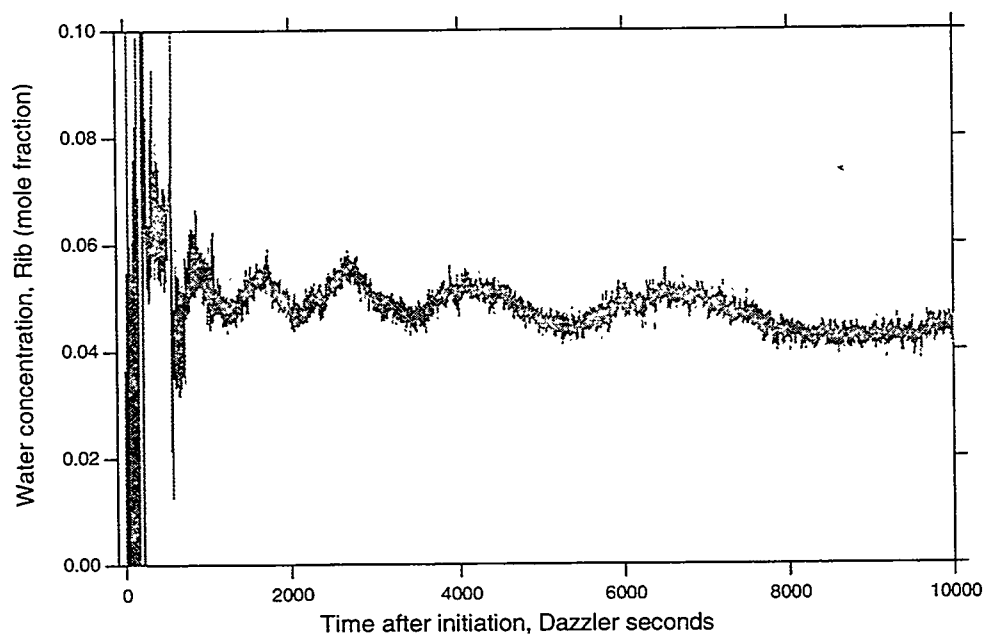
Figure F1. CO_2 measured in invert during DAZZLER.
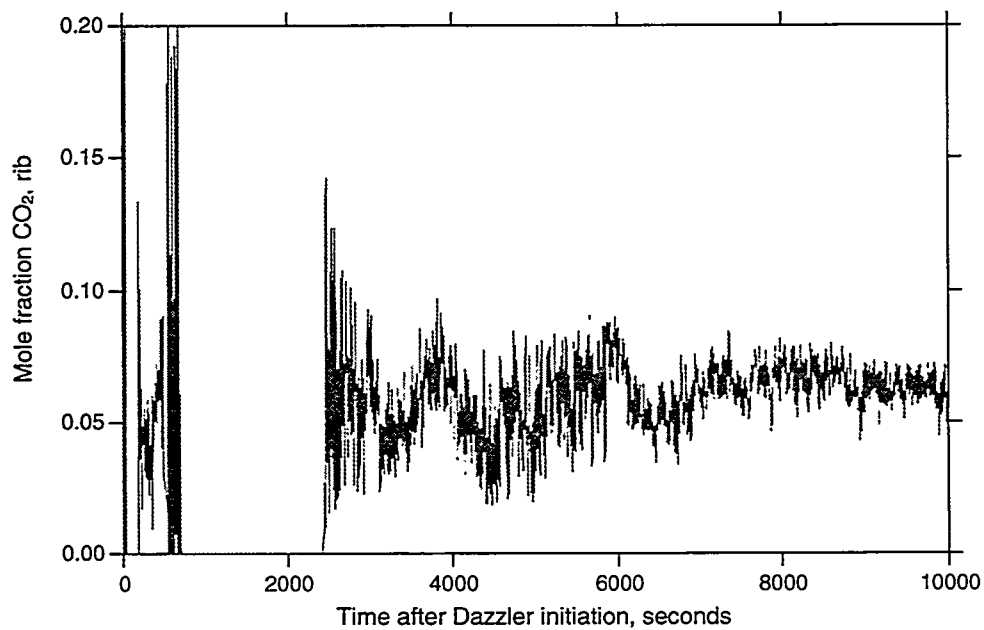
Figure F2. CO_2 measured in rib during DAZZLER.

Figure F3. Water concentration measured in rib location during DAZZLER.

APPENDIX G

Time-Resolved Measurements of Test Chamber Pressure and Gas Temperatures—LLNL and Bechtel Nevada

The pressure transients produced by the hot combustion gases mixing with and heating the ambient air in the test chamber are shown in Figure G1. The first 500 s of the data from each test are overlaid in this figure. The times to reach maximum pressure differ somewhat from test-to-test, but they correlate well with the burn times of the propellant that are observed in the video records of the tests. The characteristics of the pressure decay in each test also correlate with the cooling rates of the gases observed from the thermocouple records from each test. We note, however, that a containment seal failure in the THUNDERBIRD test resulted in a significant pressure leak at roughly the same time that the peak pressure was reached in this test. It is likely that this leak reduced the magnitude of the maximum pressure recorded in this test.

Representative temperature histories obtained from the thermocouple arrays are shown in Figures G2-G4 for the SUNSPOT, THUNDERBIRD, and DAZZLER tests, respectively. The thermocouple array used in SUNSPOT was positioned over the two motors and attached at the invert near the left rib and to the back, near the center, of the chamber. We see in Figure G2 that the thermocouples near the back of the chamber recorded extremely high temperature transients when the propellant was burning, whereas the thermocouples near the invert recorded much more gradual temperature increases. These data are consistent with the presence of significant thermal stratification in the test chamber as the gases are heated by the burning propellant. It is also evident in Figure G2 that the remnants of this stratification persist as the gases cool. Similar observations apply to the recorded temperature histories for THUNDERBIRD and DAZZLER that are shown in Figures G3 and G4, respectively. However, the thermocouple array was in a different location in the test chamber for these tests compared to its location in SUNSPOT. In THUNDERBIRD and DAZZLER, the array was oriented away from direct contact with the propellant flame and was anchored between the chamber invert and the mid-height of the chamber rib near the containment plug. The temperature variations seen in Figures G3 and G4, while still significant, are therefore not as severe as observed in Figure G2 for SUNSPOT.
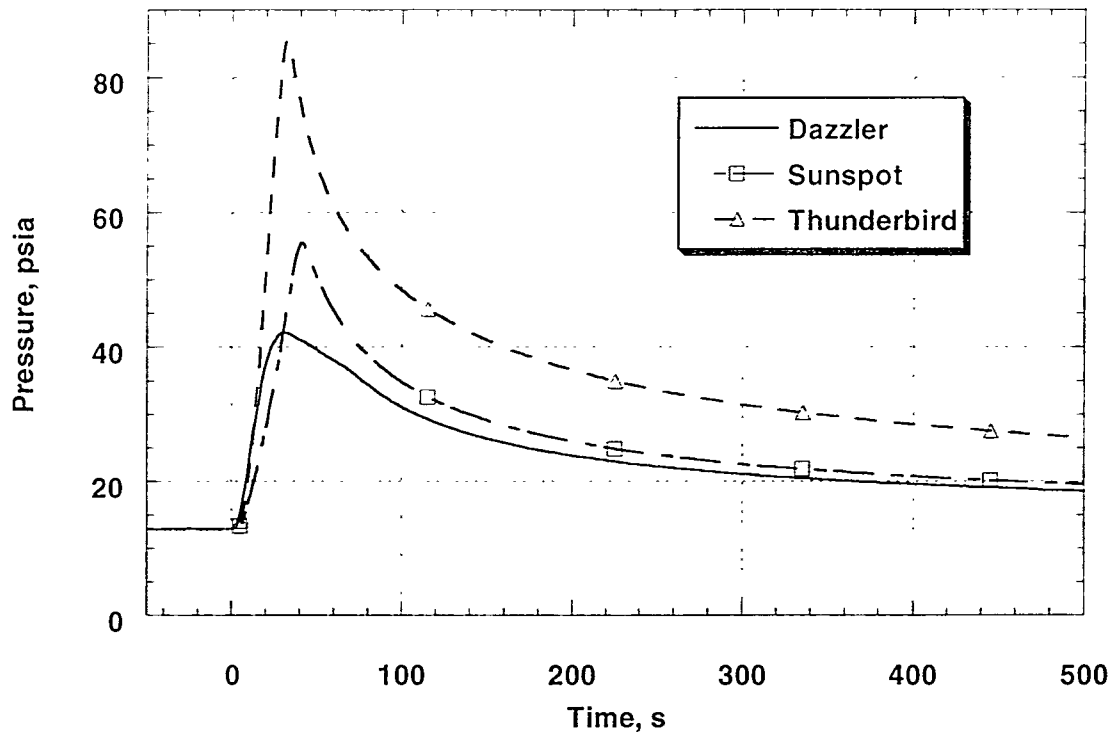
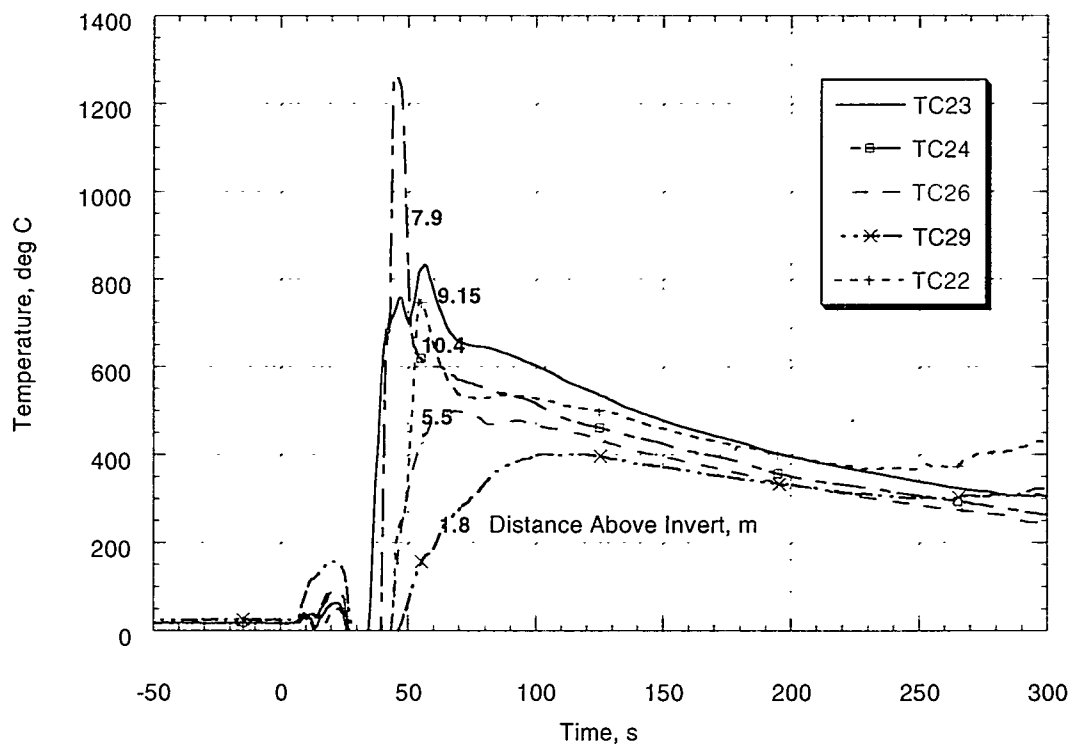**Figure G1.** Comparison of chamber pressure histories in rocket motor burn tests.

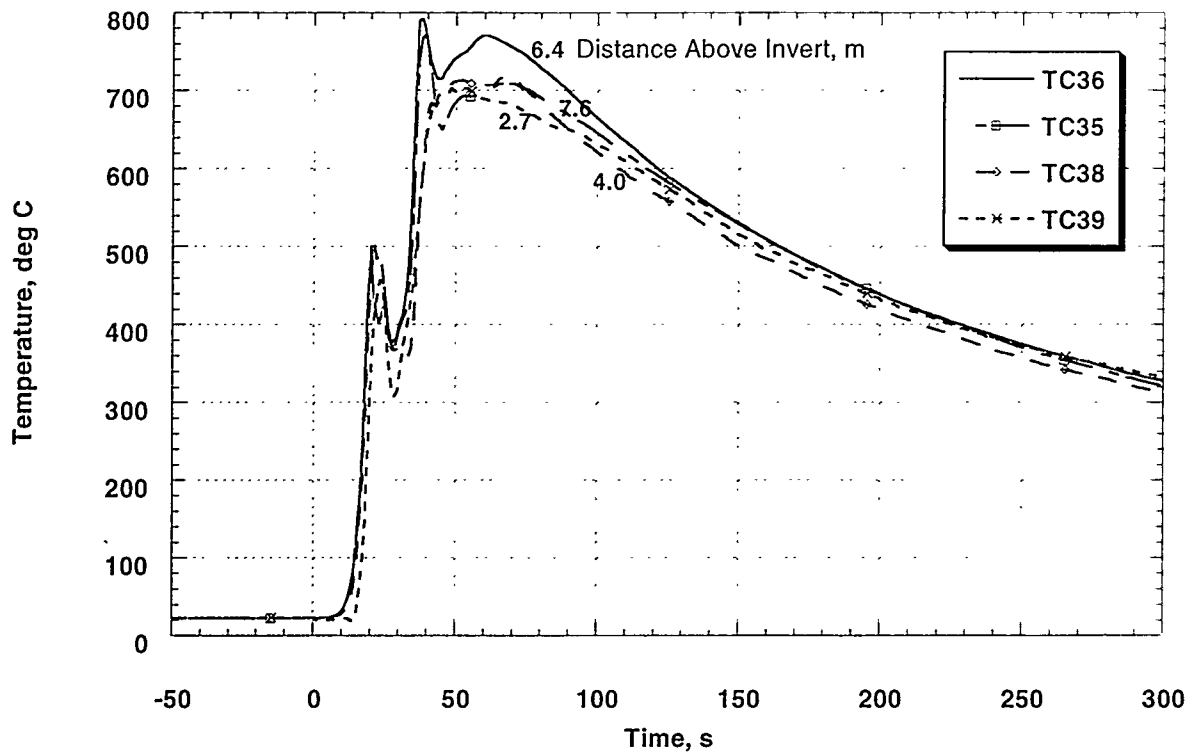**Figure G2.** Temperature histories from thermocouple array in SUNSPOT.

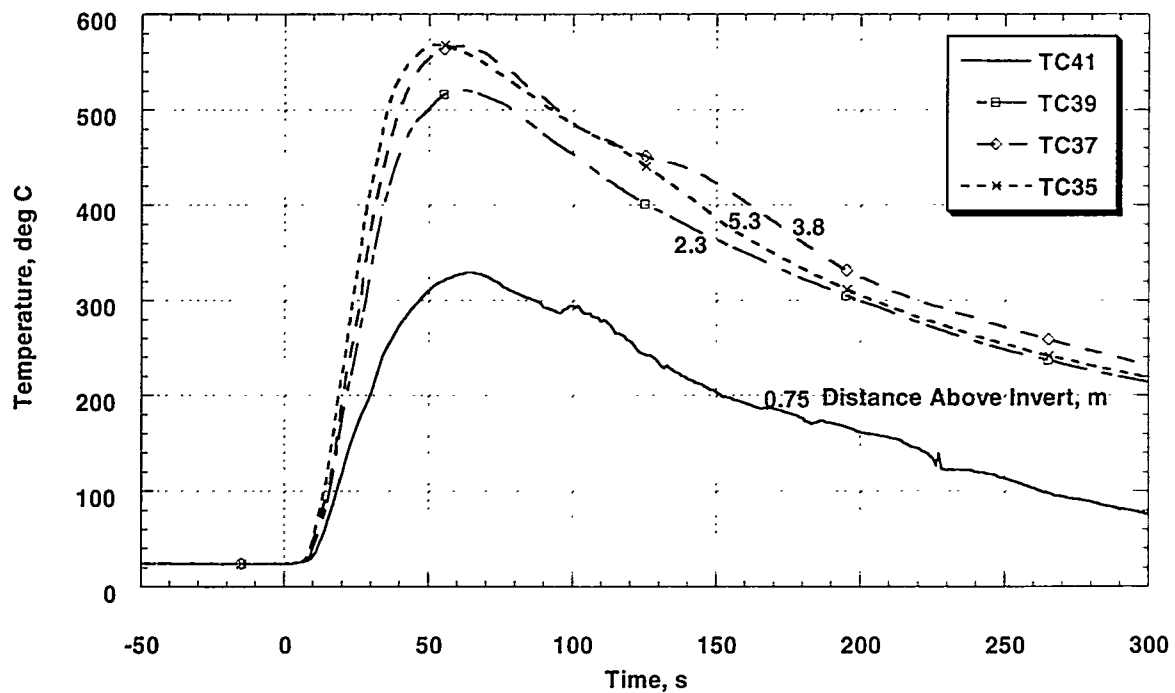**Figure G3.** Temperature histories from thermocouple array in THUNDERBIRD.

Figure G4. Temperature histories from thermocouple array in DAZZLER.

Distribution:

2   The Johns Hopkins University
Chemical Propulsion Information Agency
Attn: Jim Cocchiaro
       Tom Moore
10630 Little Patuxent Parkway, Suite 202
Columbia, MD 2104-3200

1   US Environmental Protection Agency
Attn: William Mitchell
Mail Drop 46 – ERC Annex
79 T. W. Alexander Dr
Research Triangle Park, NC 27711

4   University of California
Los Alamos National Laboratory
Attn: John Stephens, CST-1
       John Sanchez, DX-2
       Herb Fry, CST-6
       Cliff Hewitt, CST-6
P.O. Box 1663
Los Alamos, New Mexico 87545

4   University of California
Lawrence Livermore National Laboratory
Attn: Bruce Watkins, L 282
       Carol Velsko, L 231
       César Prunada, L 282
       Ray Heinle, L 221
P.O. Box 808
Livermore, CA 94550

2   Bechtel Nevada
Attn: Sam Williams
       Al Moeller
2621 Losee Road
North Las Vegas, NV 89030-4134

1   Thiokol Propulsion Group
Attn: William Munson
M/S: 130
P.O. Box 707
Brigham City, UT 84302-0689

Distribution: (continued)

1   US Department of Energy/Nevada Operations Office
Attn: Deborah Howard
P.O. Box 98518
Las Vegas, NV 89193-8518

2   University of Nevada Las Vegas
Energy Research Center
Attn: Bob Boehm
     Klaus Stezenbach
P.O. Box 454027
Las Vegas, NV 89154-4027

3   US Army Defense Ammunition Center
Attn: Jim Wheeler
     Solim Kwak
     Eddie Ansell
1 C Tree Road
McAlester, OK 74501-9002

3   Radian International LLC
Attn: John Carson
     Tim Tope
     Walt Gray
1093 Commerce Park Drive, Suite 100
Oak Ridge, TN 37830

1   Washington State University
Manufacturing-Technology Applications
Attn: Prof. Jack C. Swearengen
14204 NE Salmon Creek Ave
Vancouver, WA 98686-9600

1	9042	Bob Nilson
1	9042	Stewart Griffiths
1	9052	Don Hardesty, 8361
1	9052	Chris Shaddix, 8361
1	9052	Sarah Allendorf, 8361
1	9403	Jim Wang, 8723
1	9403	Dave Ottesen, 8723
1	9403	Howard Johnsen, 8723
1	9409	Larry Carrillo, 8421
1	9105	Jane Ann Lamph, 8119
5	9105	Joel Lipkin, 8119
1	1156	Rob Tachau, 15322
1	1157	Ray Peabody, 153221

Distribution: (continued)

1	1391	Harold Roberts, 153221
1	1167	Larry Posey, 15343
3	MS 9018	Central Technical Files, 8940-2
1	MS 0899	Technical Library, 4916
1	MS 9021	Technical Communications Department, 8528/ Technical Library, MS 0899, 4916
1	MS 9021	Technical Communications Department, 8528 For DOE/OSTI